J/ψ SPECTROSCOPY FROM MARK III*

USHA MALLIK†

Stanford Linear Accelerator Center
Stanford University, Stanford, California, 94305

Abstract

The MARK III detector at the SPEAR e^+e^- storage ring at SLAC has accumulated a data sample of 5.8×10^6 J/ψ produced. The status of the $\xi(2230)$ observed in the radiative J/ψ decay is described. The status of the glueball candidates $\eta(1440)$ $(\iota(1440))$ and $f_2(1720)$ $(\tilde{\theta}(1720))$ are probed with a systematic comparison between the radiative and the hadronic decays of J/ψ. Finally, an understanding of quark correlations is attempted from a systematic study of the J/ψ decaying into Vector-Pseudoscalar, Vector-Tensor and Vector-Scalar nonets.

Presented at the SLAC Summer Institute on Particle Physics,
Stanford, California, July 28 - August 8, 1986

* Work supported by the Department of Energy, under contracts DE-AC03-76SF00515.
† Representing the MARK III Collaboration.

1. Introduction

The discovery of charm was not only a giant step toward establishing the present standard model of electroweak interactions, but also was largely responsible for the boost in the 'religion' of QCD. A major interest and novelty in the realm of QCD has recently been to observe gluonic bound states. Such states are not accounted for in the quark model; however, according to QCD gluons are strongly interacting and they should form bound states[3] either between themselves (pure glueballs), or with the quarks and antiquarks (hybrids). The few potential candidates, which have previously been observed in radiative decays of the J/ψ,[2] [3] [4] still need to be established firmly as glueballs. The search for new candidates within this new spectroscopy continues. In a broader sense, any new physics, coming from the J/ψ, may be interesting and informative. Studies of the $\eta_c(2980)$, the charmed pseudoscalar isosinglet state into which the J/ψ decays through a magnetic dipole transition, also yield important information on charmonium decay.

In addition to the above, J/ψ decays can be used as a laboratory to study light quark spectroscopy. The initial state of J/ψ, a very sharp and narrow resonance, has a uniquely defined spin parity $J^{PC} = 1^{--}$. This, along with the low multiplicity of its decays, renders the J/ψ far more convenient for such studies than the fixed target experiments where the initial spin-parity is uncertain and the final states often contain a lot of hadronic debris.

All J/ψ decays are Okubo-Zweig-Iizuka (OZI) suppressed.[5] A large data sample of J/ψ provides the opportunity to study both the Single-OZI (SOZI) and the Double-OZI (DOZI) suppressing mechanisms. Comparison of the radiative and the hadronic decays provides not only insight into the decay mechanisms, but also helps in differentiating between the conventional $q\bar{q}$, and the 'new' spectroscopy.

The J/ψ decays into baryons provide a wealth of information about baryon interactions. Furthermore, the J/ψ, an SU(3) singlet, should hadronically decay into a baryon-antibaryon pair where both (the baryon and the antibaryon) belong to octets or both belong to the decuplets. Mixed decays where one of the two (the baryon or the antibaryon) belongs to an octet and the other to a decuplet are SU(3) forbidden. Observation of such decays, along with the SU(3) allowed decays, yields information about different couplings and their possible interference effects.

The principal decay mechanisms of the J/ψ are explained below. Figure 1 displays these in the order of strength. The mass of the J/ψ is below the charmed meson pair threshold, so direct decay into charmed mesons is forbidden. Therefore, the strong decay proceeds through (at least) three gluon exchange, as shown in Figure 1(a). (One gluon exchange is forbidden because it carries color to the final state and two gluon exchange is forbidden by charge conjugation for a color singlet.) The final state does not contain any charm quark, hence the decay is OZI suppressed. The decay strength is proportional to α_S^3, and is given explicitly by[11]

$$\Gamma(J/\psi \to 3g) = \frac{16}{9\pi}(\pi^2 - 9)\frac{5}{18}\alpha_S^3\frac{|\psi(0)|^2}{M_{J/\psi}^2} ,$$

where $\psi(0)$ is the value of the radial wavefunction of the J/ψ at the origin. This represents $\sim$ 62% of the total J/ψ branching ratios. Figure 1(b) is the electromagnetic decay through a virtual photon exchange. This is proportional to α and is calculated as

$$\Gamma(J/\psi \to e^+e^-) = 4(Q_C\alpha)^2\frac{|\psi(0)|^2}{M_{J/\psi}^2} ,$$

where $Q_C = 2/3$ is the charge of the charmed quark. This diagram represents $\sim$ 29% of the J/ψ branching ratios. Figure 1(c) is the radiative decay mechanism and has been the hunting ground for the glueball searches. The strength,

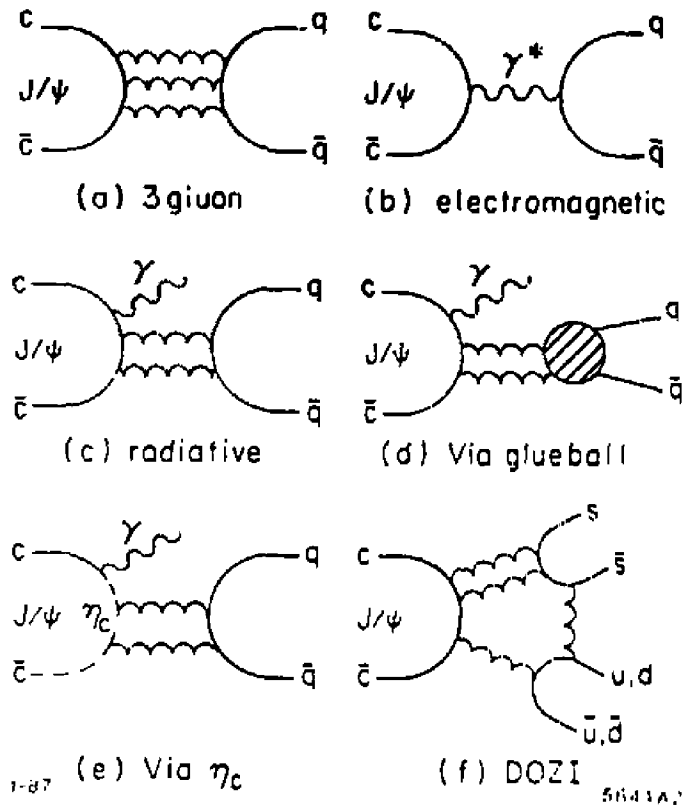

1. (*a*) Strong decay proceeding through $c\bar{c}$ annihilation into three gluons; (*b*) Electromagnetic decay through $c\bar{c}$ annihilation into one photon; (*c*) Electromagnetic decay into a final state of one photon and two gluons (radiative decay); (*d*) The two gluons forming a color singlet possible bound state (glueball); (*e*) Radiative decay through a magnetic dipole transition to η_c; (*f*) Doubly disconnected diagrams (double OZI suppression).

DISCLAIMER

proportional to $\alpha\alpha_S^2$ is calculated as[7]

$$\Gamma(J/\psi \to \gamma gg) = \frac{32}{9\pi}(\pi^2 - 9)\alpha_S^2 \alpha Q_C^2 \frac{|\psi(0)|^2}{M_{J/\psi}^2}$$

and represents $\sim$ 7% of the total J/ψ branching ratio for the radiative decay. Since the photon in the final state does not carry color, the two gluons could form a color singlet bound state. Figure 1(d) shows a possible gluonic intermediate bound state decaying into light quark mesons. It is this intermediate step that makes the radiative decays the 'hunting ground' of the 'glueball' candidates. Figure 1(e) shows a special case of a radiative decay where the J/ψ decays into an η_c through a magnetic dipole transition before the $c\bar{c}$ annihilate. This mechanism is responsible for $\sim$ 1% of the total J/ψ branching ratio and provides a very good tool for unraveling the η_c decays as mentioned earlier. Figure 1(f) shows the DOZI decay mechanism, which is comparatively small, but may not be negligible in the interference effects with other amplitudes. This is described later.

FLAVOR TAGGING:

The implications of some of these decays are explained in Fig. 2. Figure 2(a) and 2(b) show the quasi-two-body decays of the case of Fig. 1(a) and 1(b). The vector meson nonet being ideally mixed, the $\phi(1020)$ contains only strange quark *(s)*, and the $\omega(783)$ contains only up*(u)* and down*(d)* quarks. In fact the wavefunctions of these two isoscalars are, to a very good approximation,

$$\phi = |s\bar{s}>$$
$$\omega = \frac{|u\bar{u} + d\bar{d}>}{\sqrt{2}}.$$

Hence, if a ϕ (Fig. 2(a)) or an ω (Fig. 2(b)) is identified in the J/ψ decay, because of the continuation of the quark lines, the recoil system will contain the $s\bar{s}$ (Fig. 2(a)) or the $u\bar{u}$, $d\bar{d}$ (Fig. 2(b)) quark content of the respective mesons. This provides a very useful technique to determine the quark contents of various

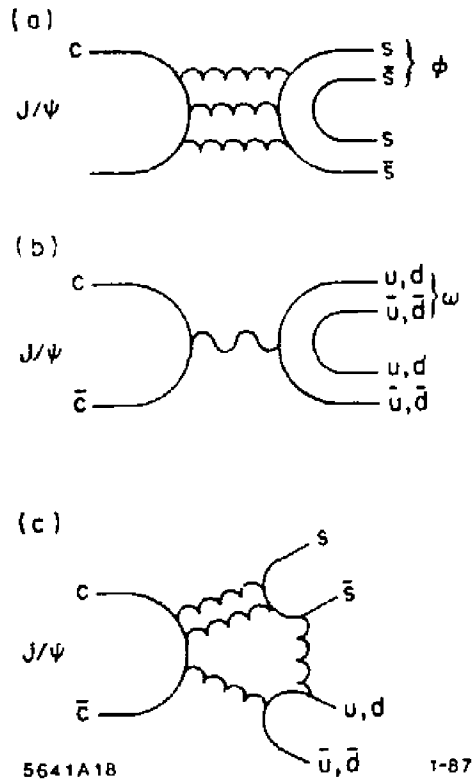

2. Quasi two-body J/ψ decay through $c\bar{c}$ annihilation into (a) a ϕ and the $s\bar{s}$ part of a meson, (b) an ω and the $(u\bar{u}+d\bar{d})$ part of a meson, (c) an $s\bar{s}$ and an $u\bar{u}, d\bar{d}$ state through DOZI mechanism.

resonances by observing their production in association with a ϕ and an ω in the J/ψ decays. This, however, is not exact because of the presence of DOZI decays, which, though small, do not obey the quark correlation as seen from Fig. 2(c).

According to the generalized G-parity[8] conservation, the J/ψ can decay hadronically into the following meson nonets

$$\begin{aligned} J/\psi \rightarrow\ & \text{Pseudoscalar (P)} + \text{Vector } (V) \\ \rightarrow\ & \text{Tensor (T)} + V \\ \rightarrow\ & \text{Scalar } (S) + V \\ \rightarrow\ & \text{Axial Vector } (A) + V \end{aligned}$$

and radiatively,

$$\begin{aligned} J/\psi \rightarrow \gamma +\ & P + P \\ & \gamma + V + V. \end{aligned}$$

The flavor tagging technique can be generalized to the whole vector nonet, where recoils against each member of the vector nonet can be studied. Such a systematic study would yield the strength of the different amplitudes e.g. strong (isospin conserving), electromagnetic (isospin violating) and SU(3) violating.

The MARK III detector at the SPEAR e^+e^- storage ring at SLAC has collected a data sample of 5.9×10^6 J/ψ produced, over two separate running periods of 1982-83 and 1985. The present paper deals with the radiative decays in Section 2, starting with the status of the $\xi(2230)$ and then searches in other radiative channels, along with the η_c decays. Section 3 deals with the status of the glueball candidate $\eta(1440)$, first observed[9] in the $K\bar{K}\pi$ mode of the radiative decay of the J/ψ. The $K\bar{K}\pi$ and $\eta\pi^+\pi^-$ channels, were studied in both radiative decays and in hadronic decays against a ϕ and an ω recoil. The controversy in the 1280 -1500 MeV/c^2 mass region over the structures $f_1(1420)/\eta(1440)$ $\{E(1420)/\iota(1440)\}$ and the $\eta(1275)/f_1(1285)$ $\{\eta(1275)/D(1285)\}$ are discussed. Section 4 describes the status of the $f_2(1720)$ in $K\bar{K}$ and $\pi^+\pi^-$ and the comparison between radiative

and hadronic decays. The quark structure of the mesons and strength of the amplitudes are determined by observing reactions of the type

$$J/\psi \rightarrow 1^{--} + 0^{-+} \quad (1)$$

$$J/\psi \rightarrow 1^{--} + 2^{++} \quad (2)$$

$$J/\psi \rightarrow 1^{--} + 0^{++} \quad (3)$$

for complete nonets. Sections 5 and 6 describe (1), an ongoing analysis of (2) and the beginning of a systematic study of (3).

2. Radiative Decays

2.1 The Status of $\xi(2230)$

MARK III reported[19] the observation of a narrow resonance $\xi(2230)$ in radiative J/ψ decay into K^+K^- in 1983, with a data sample of 2.8×10^6 produced J/ψ. Several theoretical interpretations , as to the nature of the $\xi(2220)$, were subsequently proposed e.g., a glueball or a hybrid state,[10] [11] an ordinary high spin mesonic state,[12] and others.[13] An additional statistics of 3×10^6 J/ψ from the 1985 data, confirmed[14] the previous observation. Figures 3(a) and 3(b) show the K^+K^- and the $K_S^0K_S^0$ mass spectra from the combined data sample in the radiative J/ψ decay.

Both spectra are similar in their primary features. Three clear peaks are seen in each, with the first one at $\sim$ 1525 MeV/c^2 , corresponding to the $f_2'(1525)$ $\{f'(1525)\}$, the $s\bar{s}$, $I = 0$, member of the 2^{++} nonet. (The 2^{++} nonet is almost ideally mixed.) The second peak is at $\sim$ 1720 MeV/c^2 , the $f_2(1720)\{\theta(1720)\}$, which is a prime glueball candidate[10] [14] and will be described later. The third peak (a narrow peak on top of a wide bump centered around 2100 MeV/c^2) at $\sim$ 2230 MeV/c^2 corresponds to the $\xi(2230)$. The $K_S^0K_S^0$ spectrum contains

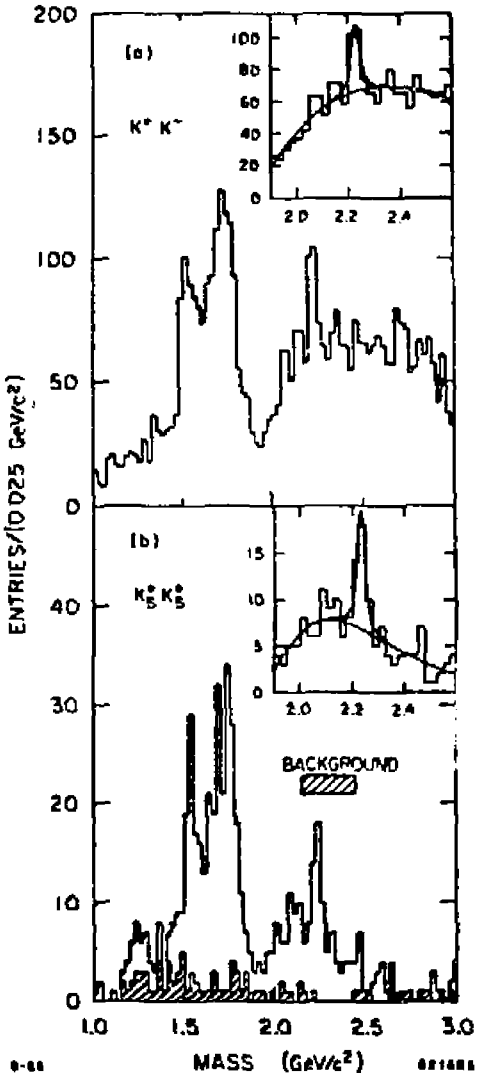

3. (*a*) K^+K^- effective mass spectrum in the radiative decay $J/\psi \to \gamma K^+K^-$, (*b*) $K_S^0K_S^0$ effective mass spectrum from the decay $J/\psi \to \gamma K_S^0K_S^0$.

little background since decays like $J/\psi \to K^0_S K^0_S \pi^0$ and $J/\psi \to K^0_S K^0_S$ are forbidden by C parity conservation. This is demonstrated in the Dalitz plots, Figures 4(a) and 4(b), for the charged and the neutral channels respectively. Diagonal bands from the above three resonances are observed ($f'_2(1525)$ and $f_2(1720)$ overlapping), as indicated in both plots. However, Fig. 4(a) contains a vertical and a horizontal band parallel to the two boundaries arising from $K^{*\pm}$ production in the reactions $J/\psi \to K^{*\pm}K^{\pm}$, misidentified as $K\bar{K}\gamma$. The accumulation of events on the two boundaries are from the misidentified decay $J/\psi \to e^+e^-\gamma$.

A maximum likelihood fit of a Breit-Wigner line shape in the 1900-2600 MeV/c^2 region yielded the parameters of the $\xi(2230)$ as

$$m(\xi) = 2230 \pm 6 \pm 14 \quad \mathrm{MeV}/c^2$$
$$\Gamma(\xi) = 26^{+20}_{-10} \pm 17 \quad \mathrm{MeV}/c^2$$

for the charged mode, and,

$$m(\xi) = 2232 \pm 7 \pm 7 \quad \mathrm{MeV}/c^2$$
$$\Gamma(\xi) = 18^{+23}_{-15} \pm 10 \quad \mathrm{MeV}/c^2$$

for the neutral mode. The first error corresponds to the statistical and the second error corresponds to the systematic error. The measured branching ratios of the two decay modes were

$$B(J/\psi \to \gamma\xi) \cdot B(\xi \to K^+K^-) = (4.2^{+1.7}_{-1.4} \pm 0.8) \times 10^{-5}$$
$$\text{and } B(J/\psi \to \gamma\xi) \cdot B(\xi \to K^0_S K^0_S) = (3.1^{+1.6}_{-1.3} \pm 0.7) \times 10^{-5}\ .$$

The ratio of the branching ratios is consistent with the $\xi(2230)$ being an isoscalar. Details have been presented elsewhere.[14]

A preliminary spin-parity analysis, using a maximum likelihood technique, has been performed in the relatively background free $K^0_S K^0_S$ mode, to determine

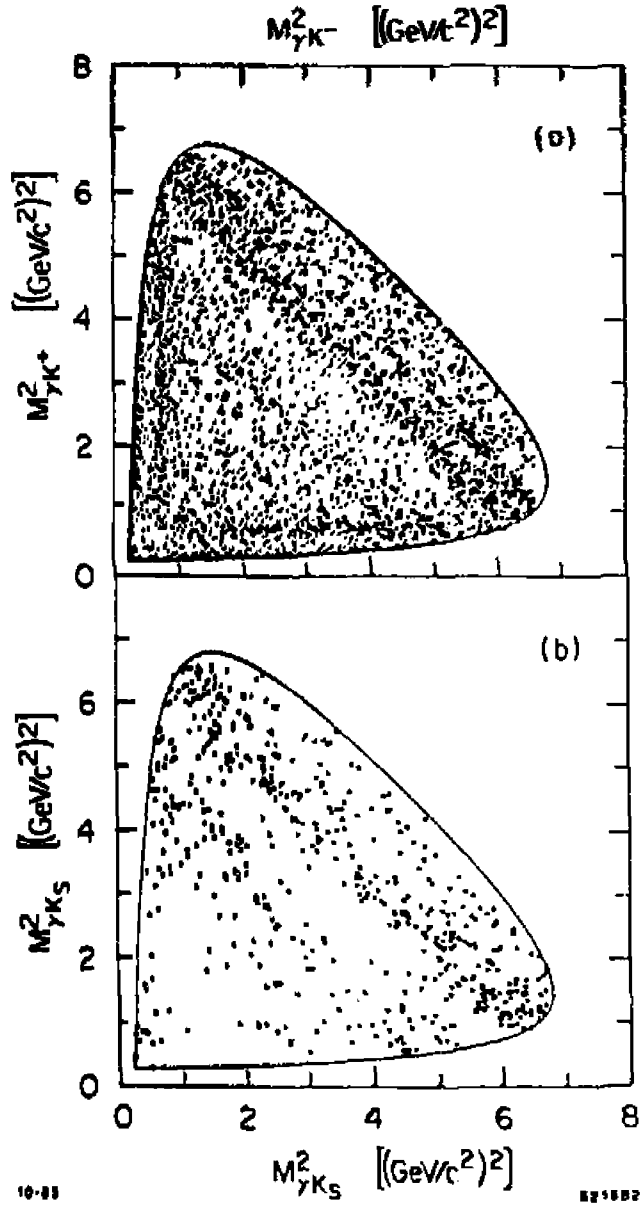

4. Dalitz plot distributions for the decays (*a*) $J/\psi \to \gamma K^+K^-$ and (*b*) $J/\psi \to \gamma K^0_S K^0_S$.

the J^P of the $\xi(2230)$. This maximum likelihood technique using the helicity amplitudes was employed earlier[17] to determine the spin-parity of the $f_2'(1525)$ and the $f_2(1720)$ with a smaller data sample. Figure 5 (a),(b),(c) show the $\cos\theta_{K_S^0}$ distributions for the $f_2'(1525)$ region [1420-1550 MeV/c^2], $f_2(1720)$ region [1620-1820 MeV/c^2] and the $\xi(2230)$ region [2180-2280 MeV/c^2] respectively, where $\theta_{K_S^0}$ is the polar angle, with respect to the photon direction of one of the K_S^0's in the $K_S^0K_S^0$ center-of-mass frame. The spins determined for both the $f_2'(1525)$ and the $f_2(1720)$ were 2 (the $K_S^0K_S^0$ system can only have even spin and positive parity, i.e., 0^+, 2^+, $4^+\ldots$). The analysis assigned a minimum spin of 2 to ξ, although a spin 4 assignment could not be excluded.[18] (The effect of the 2100 MeV/c^2 region was examined separately and its contribution was estimated as well as possible.) Due to the meager statistics a full Partial Wave Analysis (PWA) was not performed.

The DM2 collaboration, with a data sample of 8.6×10^6 produced J/ψ, reported[19] the lack of observation of a narrow resonance near 2210 MeV/c^2. However, the GAMS collaboration has presented evidence[20] for a narrow structure in $\eta\eta'$ at $\sim$ 2220 MeV/c^2 with $J^P \geq 2^+$, in the reaction

$$\pi^- p \to \eta\eta' + n$$

at 38 and 100 GeV/c.

The LASS collaboration also reported[21] observation of a state at $\sim$ 2200 MeV/c^2 decaying into $K_S^0K_S^0$ and K^+K^- in the reactions

$$K^- P \to \Lambda K_S^0 K_S^0 \quad \text{and} \quad K^- P \to \Lambda K^+ K^-$$

at 11 GeV/c. A moment analysis prefers the spin-parity of this state to be 4^{++}.

The search for other decay modes of the $\xi(2230)$ by MARK III and the upper limits in various channels have been previously presented.[16]

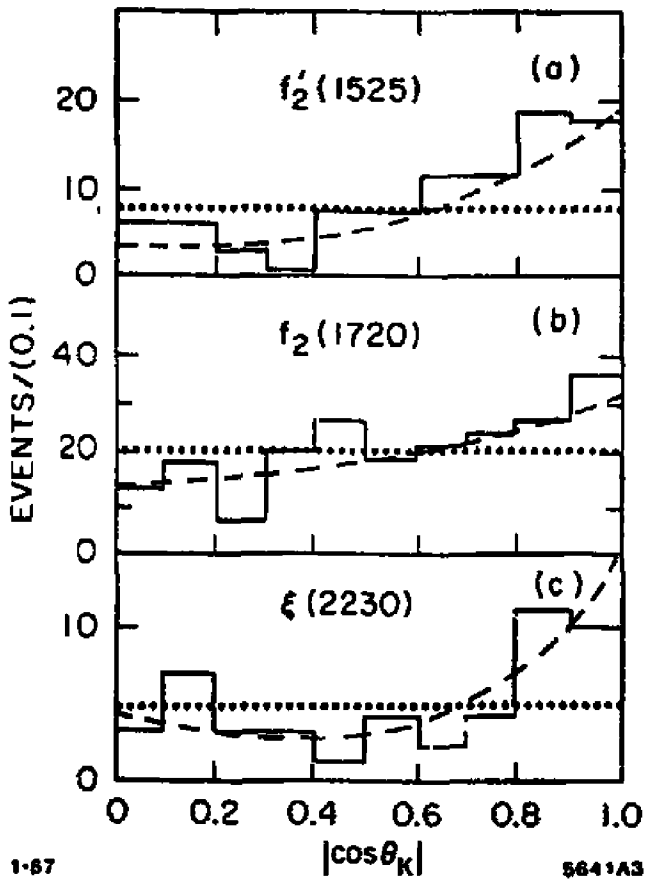

5. The $\cos\theta_K$ distributions for events in the region (a) 1420-1550 MeV/c^2, (b) 1620-1820 MeV/c^2, and (c) 2180-2280 MeV/c^2. The histograms are the data. The dotted lines are the Monte Carlo predictions for the spin 0 and the dashed lines for the spins 2 hypotheses.

2.2 $J/\psi \to \gamma\phi\phi$

Three glueball candidates were reported[22] to decay into $\phi\phi$ in the fixed target reaction $\pi^- p \to \phi\phi + n$. Hence the $\xi(2230)$ was searched for in the radiative $\phi\phi$ decay of the J/ψ. The observation of the $\eta_c(2980)$ decay into $\phi\phi$ in the reaction

$$J/\psi \to \gamma\,\phi \quad \phi$$
$$\qquad\quad \lfloor\!\to K^+K^- \;\; \lfloor\!\to K^+K^-$$

was published[23] earlier by MARK III with a smaller data sample. Recently, the DM2 collaboration has published their results in this decay mode.[24]

The $\phi\phi$ effective mass distribution is plotted in Fig. 6(a); the evidence for $\phi\phi$ production from the four charged kaons is shown in the scatter plot in Fig. 6(b). Figure 6(a) shows clear production of the $\eta_c(2980)$, while the lower mass region around 2200-2400 MeV/c^2 shows interesting structures. The charged kaon detection efficiency in the lower mass region is critical because of the kinematics. A careful evaluation of the efficiency and detection of the ϕ in decay modes e.g., $K^0_S K^0_L$ and $\pi^+\pi^-\pi^0$, which do not suffer from similar problems, are underway. Presently, the branching ratio in the $\phi\phi$ mass region of 2100-2400 MeV/c^2 is measured to be

$$B(J/\psi \to \gamma\phi\phi) \;=\; (4.0 \pm 0.5 \pm 0.8) \times 10^{-4}.$$

The spin-parity of the relevant structures are also being examined.

2.3 $J/\psi \to \gamma\omega\phi$

One of the proposed decay modes of a hybrid[10] $\xi(2230)$, is thought to be $\omega\phi$. An additional motivation for studying this decay mode was to complete a systematic study of the $\eta_c \to 1^{--}1^{--}$ decays, which was published[25] earlier (with the smaller data sample), without the $\omega\phi$ mode. The various decay

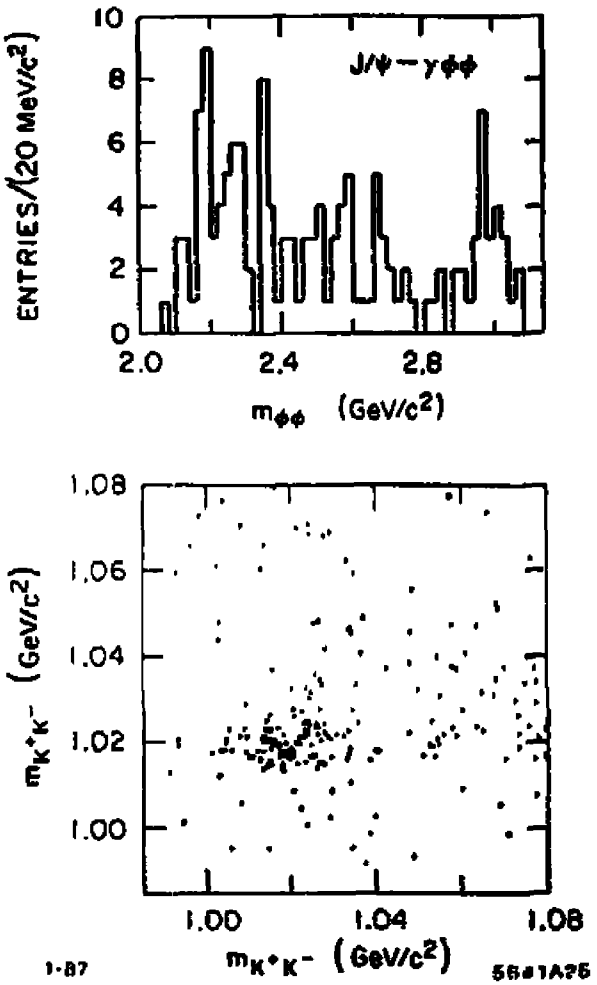

6. (a) $\phi\phi$ mass spectrum from the reaction $J/\psi \to \gamma\phi\phi \to \gamma 4K^{\pm}$, (b) Scatter plot of K^+K^- vs K^+K^-.

mechanisms of the $\eta_c(2980)$ are shown in Fig. 7(a). It was suggested[24] that the measurement of this decay mode would yield important insight into the relevant diagrams contributing to the $\eta_c(2980)$ decay. If flavour - SU(3) were exact, the reduced branching ratios $\tilde{B}(\eta_c \to \phi\phi)$, $\tilde{B}(\eta_c \to \rho^0\rho^0)$, $\tilde{B}(\eta_c \to \omega\omega)$, and $\frac{1}{2}\tilde{B}(\eta_c \to K^{*0}\bar{K}^{*0})$ should all be equal. These measurements are being repeated with the present high statistics data.

Figure 7(b) shows the $\omega\phi$ effective mass plot in the decay,

$$J/\psi \to \gamma\,\omega\,(\to \pi^+\pi^-\pi^0)\;\phi\,(\to K^+K^-).$$

A hint of the $\xi(2230)$ is visible with a few events at 2230 MeV/c^2. An upper limit was estimated with a conservative approach,

$$B(J/\psi \to \gamma\xi(2230)) \cdot B(\xi(2230) \to \omega\phi) < 5.9 \times 10^{-5},$$

at a 90% C.L. Note for comparison that the branching ratios of the J/ψ into K^+K^- and $K^0_SK^0_S$ are

$$B(J/\psi \to \gamma\xi(2230)) \cdot B(\xi(2230) \to K^+K^-) = (4.2^{+1.7}_{-1.4} \pm 0.8) \times 10^{-5},$$

and

$$B(J/\psi \to \gamma\xi(2230)) \cdot B(\xi(2230) \to K^0_SK^0_S) = (3.1^{+1.6}_{-1.3} \pm 0.7) \times 10^{-5}.$$

No signal for the $\eta_c(2980)$ is visible. The upper limit at 90% C.L. is

$$B(J/\psi \to \gamma\eta_c(2980)) \cdot B(\eta_c(2980) \to \omega\phi) < 1.3 \times 10^{-5}$$

The inclusive branching ratio into $\gamma\omega\phi$ was measured as

$$B(J/\psi \to \gamma\omega\phi) = (1.40 \pm 0.25 \pm 0.28) \times 10^{-4}.$$

In summary,

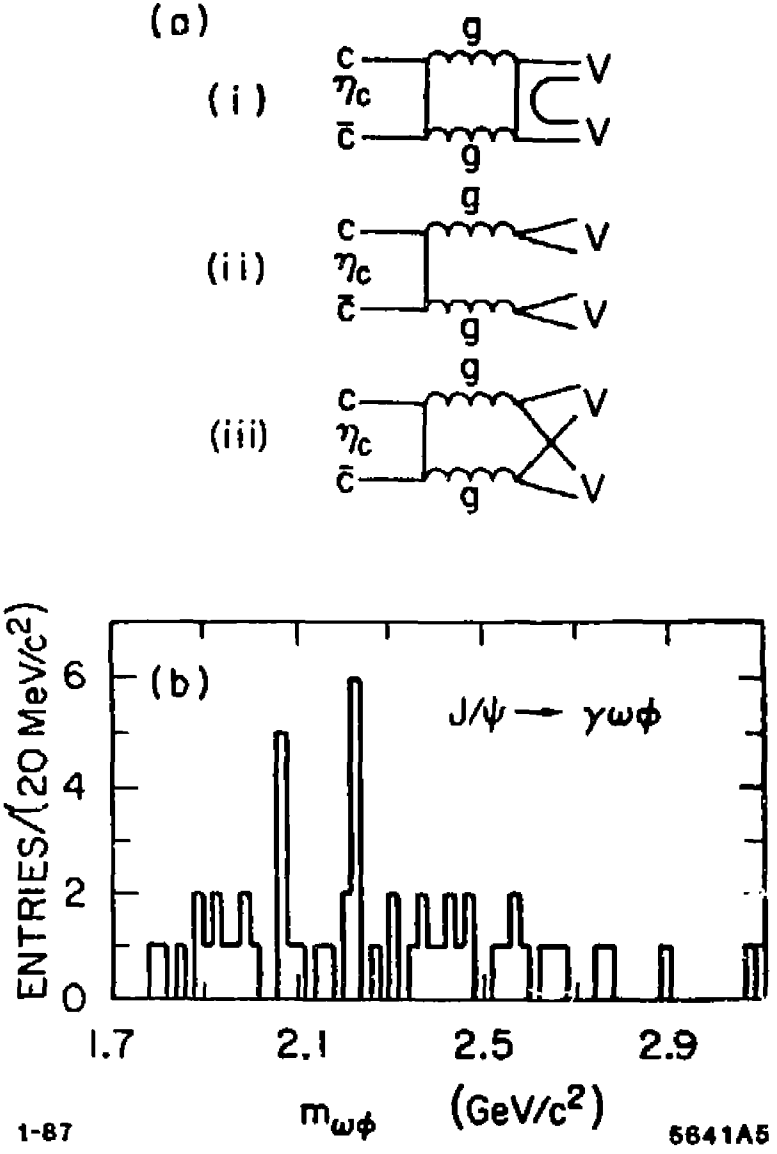

7. (*a*) Mechanisms for $\eta_c \rightarrow VV$ decay. In (ii) the produced mesons are color-octet states, but supposedly turn into color singlets by soft gluon exchanges, i.e. final state interactions. (*b*) $\omega\phi$ mass spectrum from the reaction $J/\psi \rightarrow \gamma\omega\phi$.

i) The narrow state $\xi(2230)$, first observed by MARK III has been established. The spin-parity determination by a maximum likelihood fit to the helicity amplitudes favors $J^P \geq 2^+$.

ii) The $\eta_c(2980)$ was observed in the $\phi\phi$ decay mode with increased statistics in an ongoing analysis of $J/\psi \rightarrow \gamma\phi\phi$. The mass region between 2200-2400 MeV/c^2 shows interesting structures.

iii) The radiative decay $J/\psi \rightarrow \gamma\omega\phi$ was observed with a few events at 2230 MeV/c^2 . No significant $\eta_c(2980)$ signal was observed. A complete analysis of $\eta_c \rightarrow 1^{--}1^{--}$ with increased statistics is underway and should yield important insight into the decay mechanism.

3. The 1400 - 1500 MeV/c^2 Region and the 1280 MeV/c^2 Region

The 'old' and the 'new' spectroscopy came to meet in a bitter feud in the 1400-1500 MeV/c^2 mass region. The $f_1(1420)$ $\{E(1420)\}$ has been around for over twenty years as a member of the 1^{++} axial vector nonet, primarily containing $s\bar{s}$ quarks.[28] However, a recent high statistics PWA[27] claimed the spin-parity of the $f_1(1420)$ to be 0^{-+}. The $\eta(1440)$, a pseudoscalar glueball candidate, was and has been observed in radiative J/ψ decays. As mentioned earlier, while the radiative decays could be the ideal place to look for glueballs, the ordinary $q\bar{q}$ mesons are also observed here. Therefore, with the possibility of the $f_1(1420)$ being a pseudoscalar, it has been suggested[28] that the $f_1(1420)$ is the same as, or part of, the $\eta(1440)$. To address this question, the radiative decay $J/\psi \rightarrow \gamma K\bar{K}\pi$ was compared with the hadronic decays, $J/\psi \rightarrow \omega K\bar{K}\pi$, and $J/\psi \rightarrow \phi K\bar{K}\pi$.

The $K\bar{K}\pi$ Decay Mode

3.1 $J/\psi \to \gamma K\bar{K}\pi$

The $\eta(1440)$ was observed by MARK III in the decay modes $J/\psi \to \gamma K^{\pm} K_S^0 \pi^{\mp}$, and $J/\psi \to \gamma K^+ K^- \pi^0$ and a complete Dalitz plot analysis was performed[20] with the earlier data sample. The spin-parity of the $\eta(1440)$ was determined to be 0^-, and the mass and the width

$$m = 1456 \pm 5 \pm 6 \quad \text{MeV}/c^2$$
$$\Gamma = 95 \pm 10 \pm 15 \quad \text{MeV}/c^2$$

in $K^{\pm} K_S^0 \pi^{\pm}$ mode, and

$$m = 1461 \pm 5 \pm 5 \quad \text{MeV}/c^2$$
$$\Gamma = 101 \pm 10 \pm 10 \quad \text{MeV}/c^2$$

in $K^+ K^- \pi^0$ mode. The measured branching ratios were

$$B(J/\psi \to \gamma\eta(1440)) \cdot (\eta(1440) \to K^{\pm} K_S^0 \pi^{\mp}) = (16.5 \pm 1.0 \pm 2.7) \times 10^{-4}$$

and,

$$B(J/\psi \to \gamma\eta(1440)) \cdot (\eta(1440) \to K^+ K^- \pi^0) = (8.2 \pm 0.4 \pm 1.4) \times 10^{-4} .$$

These are in agreement with the isospin zero prediction of 2:1. The branching ratio into $K\bar{K}\pi$, corrected for the unseen decay modes was

$$B(J/\psi \to \gamma\eta(1440)) \cdot (\eta(1440) \to K\bar{K}\pi) = (50 \pm 3.0 \pm 8.0) \times 10^{-4} .$$

Figure 8 (a), (b) and (c) show the $K^{\pm} K_S^0 \pi^0$, $K^+ K^- \pi^0$ and the $K_S^0 K_S^0 \pi^0$

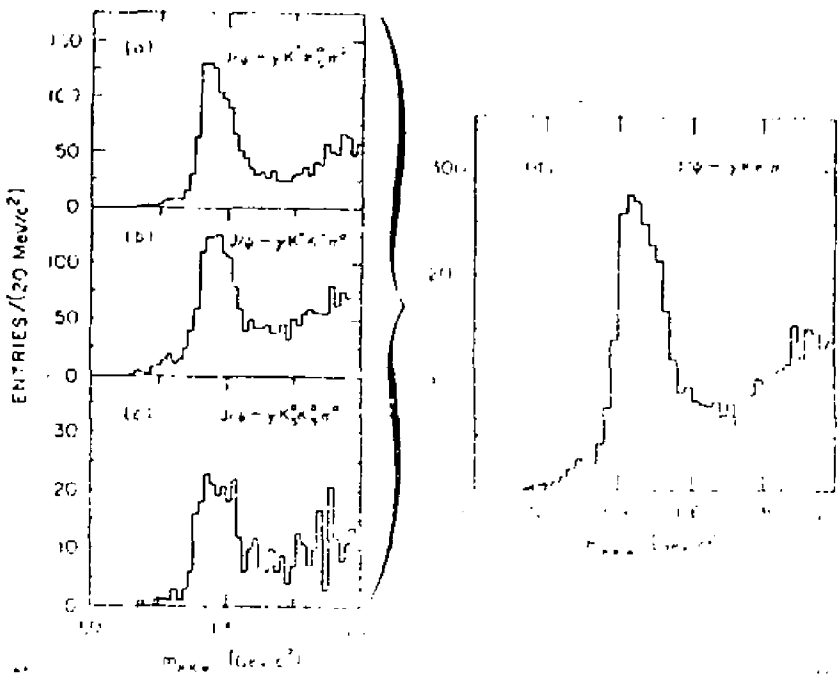

8. The $\eta(1440)$ signal in $K\bar{K}\pi$ from the decay modes (*a*) $J/\psi \to \gamma K^{\pm} K_S^0 \pi^{\mp}$, (*b*) $\gamma K^+ K^- \pi^0$, (*c*) $\gamma K_S^0 K_S^0 \pi^0$, and (*d*) the sum of the three, $J/\psi \to \gamma K\bar{K}\pi$.

effective mass spectra respectively from the reactions

$$J/\psi \rightarrow \gamma K^{\pm} K_S^0 \pi^{\mp}$$
$$J/\psi \rightarrow \gamma K^+ K^- \pi^0$$
$$and \;\; J/\psi \rightarrow \gamma K_S^0 K_S^0 \pi^0$$

from the recent high statistics J/ψ data sample. Clear peaks at $\sim$ 1440 MeV/c^2 are observed in all three spectra. However, they could not be described well by a simple Breit-Wigner parametrization of the data. Figure 8(d) shows the three spectra combined. The $K\bar{K}\pi$ final states can arise from either $K^*(892)K$ or $a_0(980)$ $\{\delta(980)\}\pi$ intermediate states. In the $K^*(892)K$ mode, the threshold effect can be important. To observe possible substructures, the $\eta(1440)$ peak was split into a lower [1360-1460 MeV/c^2] and an upper mass [1460-1580 MeV/c^2] band. Figure 9(a) and (b) show the Dalitz plots for these two mass regions. In the upper mass region, away from the $K^*(892)K$ threshold, the Dalitz plot indicates presence of the $K^*(892)$. In the lower mass region, kinematic effects make it hard to distinguish between the two isobars $K^*(892)$ and the $a_0(980)$. In addition, the $a_0(980)$ decays mostly into $\eta\pi$ and partially into $K\bar{K}$ which is suppressed by phase space. Hence, one has to keep in mind that the observed spectrum can be the result of a threshold effect, a coupled channel effect or possible interferences between different intermediate states. A complete PWA program is necessary to unfold the spectrum and such a study is underway.

3.2 $J/\psi \rightarrow \omega + K\bar{K}\pi$ *and* $\phi + K\bar{K}\pi$

As mentioned earlier, the $q\bar{q}$ mesons are copiously produced in the hadronic decays of the J/ψ. The $f_1(1420)$, was first seen [20] in $p\bar{p}$ annihilations at rest in the $K\bar{K}\pi$ decay mode, and its spin-parity was assigned to the be 0^-. Its subsequent observations in hadroproduction experiments showed[31] [32] the state to have a $J^{PC} = 1^{++}$ and a dominant K^*K decay[31] mode. Some recent experiments observed the $f_1(1420)$ decay into $K\bar{K}\pi$[27] and $\eta\pi\pi$[33] through a $a_0(980)\pi$

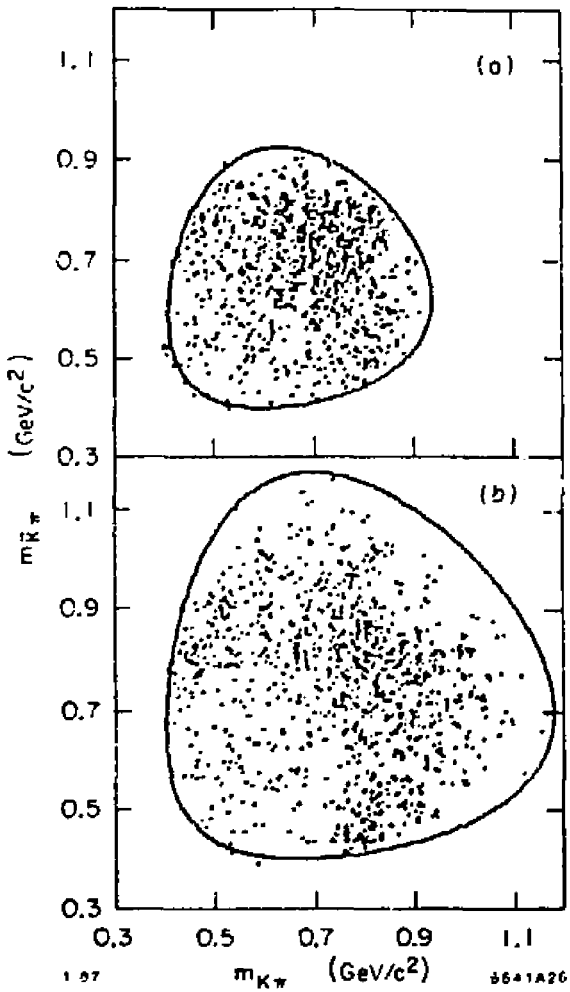

9. Dalitz plot distribution of the events in the $\eta(1440)$ region of (*a*) 1360-1460 MeV/c^2 and (*b*) 1460-1580 MeV/c^2 .

intermediate state. So, comparing the resonance structures in the final states $K\bar{K}\pi$ and $\eta\pi\pi$ produced in radiative decays and in association with a ϕ and an ω in hadronic decays of the J/ψ, address the following questions at the same time; *i*) do we see the $\eta(1440)$ in hadronic decays, *ii*) is $f_1(1420)$ distinct from the $\eta(1440)$, and iii) what is the $f_1(1420)$.

3.3 $J/\psi \to \omega K\bar{K}\pi$

The following decay modes were observed;

$$J/\psi \to \omega K^+ K^- \pi^0 \quad \Big\lfloor_{\to\, \pi^+\pi^-\pi^0} \qquad i)$$

and,

$$J/\psi \to \omega K^\pm K^0_S \pi^\mp \quad \Big\lfloor_{\to\, \pi^+\pi^-\pi^0} \qquad ii)$$

Figure 10(a) and (b) show the reconstructed $\pi^+\pi^-\pi^0$ spectra from *i*) and *ii*) respectively. Clean ω signals are visible in both cases.

Figure 11(a) and (b) show the $K^+K^-\pi^0$ invariant mass from *i*) and the $K^+K^0_S\pi^\pm$ invariant mass from *ii*) recoiling against the ω.

The spectra are very similar in nature. Figure 11(c) contains the sum of 11(a) and (b).* A clear peak at $\sim$ 1440 MeV/c^2 is observed. Analysis of *i*) and *ii*) was first performed separately, and then together; they were found to be consistent with each other. Details are given elsewhere.[104] Fitting the combined spectrum with a Breit-Wigner (and a polynomial background), one obtains the

* The background from events not containing a ω (marked by the shaded area) is estimated from observing the $K\bar{K}\pi$ events associated with the events from the sidebands of the ω.

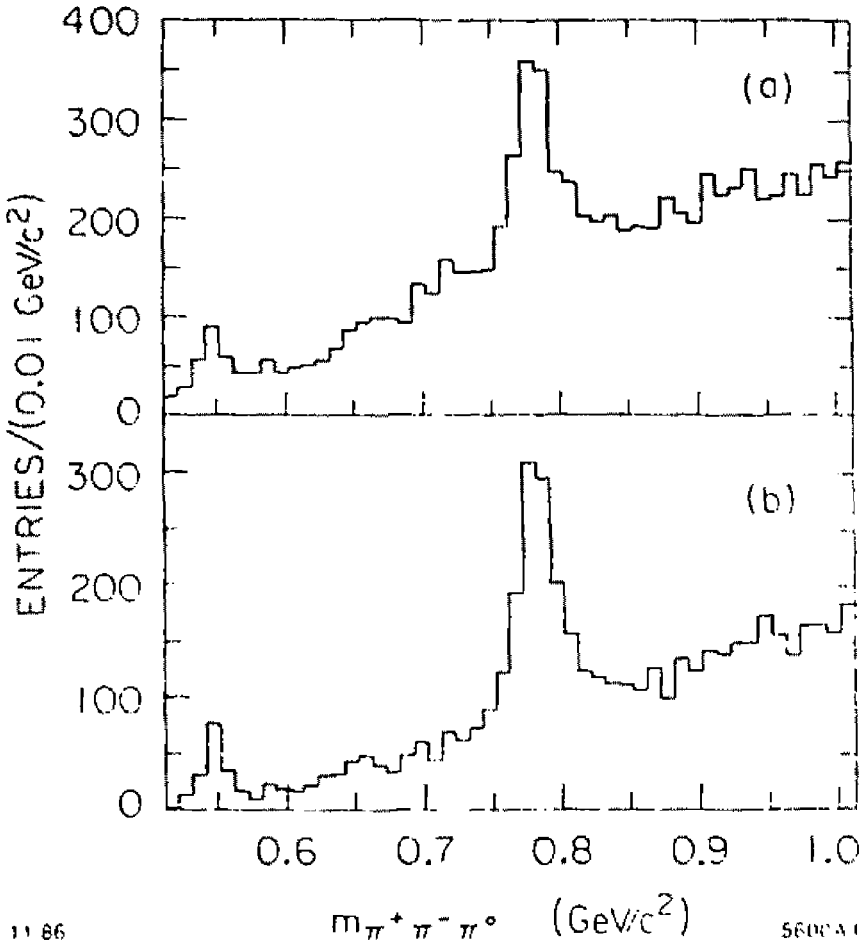

Fig. 10. The $\pi^+\pi^-\pi^0$ invariant mass distributions from the reactions (a) $J/\psi \to \omega K^+K^-\pi^0$ with two possible entries per event and (b) $J/\psi \to \omega K^+K^0_S\pi^-$ with six possible entries per event.

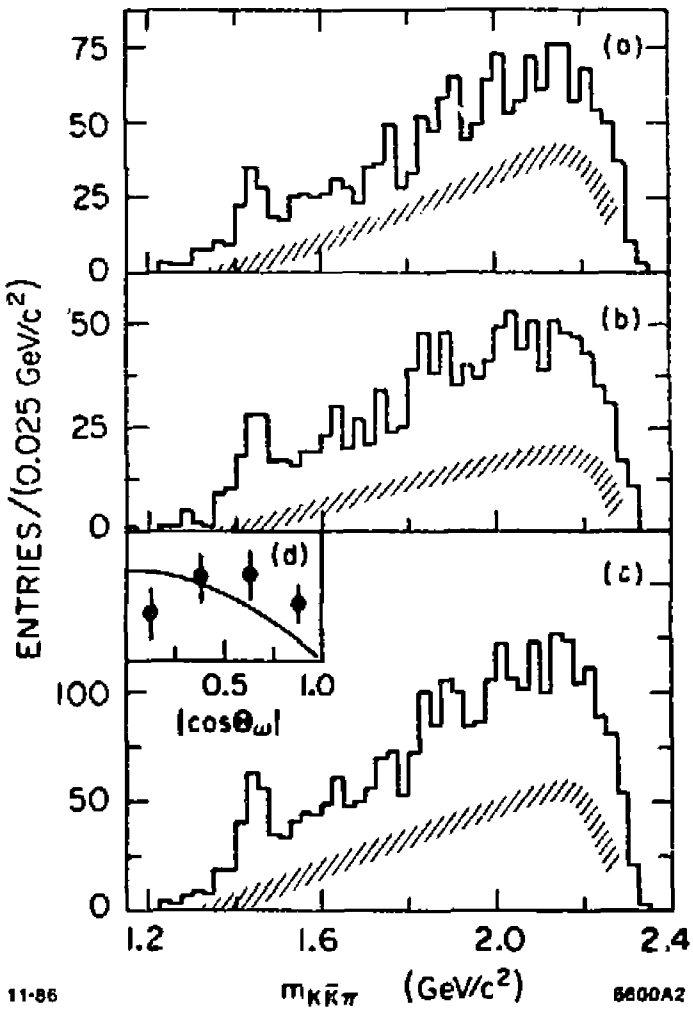

11. (*a*) $K^{\pm}K^{0}_{S}\pi^{\mp}$ invariant mass distribution from the reaction $J/\psi \rightarrow \omega K^{\pm}K^{0}_{S}\pi^{\mp}$, (*b*) $K^{+}K^{-}\pi^{0}$ invariant mass distribution from $J/\psi \rightarrow \omega K^{+}K^{-}\pi^{0}$, and (c) the sum of the two. The shaded bands show the estimate of the background. (*d*) distribution of $|\cos\theta_{\omega}|$ with prediction.

mass and the width of the peak,

$$m = 1442 \pm 5^{+10}_{-17}\ \mathrm{MeV/c^2}$$
$$\Gamma = \ \ 40^{+17}_{-13} \pm 5\ \mathrm{MeV/c^2}$$

The width, which is given as $24 < \Gamma < 84\ \mathrm{MeV/c^2}$ at a 90% C.L., is not consistent with that of the $\eta(1440)$.[34] Table 1 lists the relevant branching ratios, as well as the results of the Breit-Wigner fits for each decay mode individually and combined. The angular distribution of the ω, recoiling against the 1440 $\mathrm{MeV/c^2}$ peak was studied in order to distinguish between 0^- and 1^+ of the spin-parity of the state. Figure 11(d) shows the distribution of the normal to the ω decay plane in the helicity system of the ω. The solid curve is the prediction for a $J^P = 0^-$ state. The data clearly is very different from the pseudoscalar assumption (a fit yields a 6% probability). A coupled channel analysis[35] was performed to the $K\bar{K}\pi$ system assuming that the $K\bar{K}\pi$ consisted of three contributions, *i*) a K^*K intermediate state, *ii*) an $a_0(980)\pi$ intermediate state, and *iii*) an isotropic distribution. The K^*K was observed to be the dominant contribution and the resonant structure was assigned a $J^P = 1^+$ by this technique. If the DOZI contributions were neglected, the $f_1(1420)$, an axial-vector-like object, produced in association with an ω in J/ψ hadronic decay should have a substantial amount of u, d quark content.

3.4 $J/\psi \to \phi K\bar{K}\pi$

The following decay modes were examined,

$$J/\psi \to \phi \quad K^+K^-\pi^0 \qquad i)$$
$$\qquad\quad \lfloor\!\rightarrow K^+K^-$$

and

TABLE 1. Measured Branching Ratios into $K\bar{K}\pi$ and $\eta\pi\pi$ Decay Modes

Decay mode $J/\psi \to$	Object	Mass MeV/c^2	Width MeV/c^2	Branching Ratio $\times 10^{-4}$
				$(J/\psi \to \gamma\eta(1440)) \cdot (\eta(1440) \to K\bar{K}\pi)$
$\gamma + K^{\pm}K^0_S\pi^{\mp}$ †	$\eta(1440)$	$1456 \pm 5 \pm 6$	$95 \pm 10 \pm 15$	$= 50 \pm 3 \pm 8$
$\gamma + K^+K^-\pi^0$ †		$1461 \pm 5 \pm 5$	$101 \pm 10 \pm 10$	$= 49 \pm 2 \pm 8$
$\omega + K^{\pm}K^0_S\pi^{\mp}$	inclusive	inclusive	inclusive	$29.5 \pm 1.4 \pm 7.0$
$\omega + K^0\bar{K} + cc$	inclusive	inclusive	inclusive	$53 \pm 14 \pm 14$
				$(J/\psi \to \omega' f_1(1420)')$
$\omega + K^{\pm}K^0_S\pi^{\mp}$	$'f_1(1420)'$	$1442 \pm 7^{+10}_{-17}$	$44^{+22\ +12}_{-16\ -5}$	$\cdot('f_1(1420)' \to K^{\pm}K^0_S\pi^{\mp}) = 2.1^{+0.8}_{-0.7} \pm 0.6$
$\omega + K^+K^-\pi^0$		$1440 \pm 7^{+10}_{-17}$	$34^{+22}_{-16} \pm 5$	$\cdot('f_1(1420)' \to K^+K^-\pi^0) = 1.3^{+0.5}_{-0.4} \pm 0.3$
$\omega + K\bar{K}\pi$		$1442 \pm 5^{+10}_{-17}$	$40^{+17}_{-13} \pm 5$	$\cdot('f_1(1420)' \to K^+K^-\pi^0) = 6.8^{+1.9}_{-1.6} \pm 1.7$
$\phi + K^{\pm}K^0_S\pi^{\mp}$	inclusive	inclusive	inclusive	$= 7.0 \pm 0.6 \pm 1.0$
$\phi + K\bar{K}\pi$	$'f_1(1420)'$	1420-1440	40-60	$(J/\psi \to \phi' f_1(1420)') \cdot ('f_1(1420)' \to K\bar{K}\pi) < 1.2$ @ 90% C.L.
$\phi + K\bar{K}\pi$	$'\eta(1440)'$	1460	92	$(J/\psi \to \phi'\eta(1440)') \cdot ('\eta(1440)' \to K\bar{K}\pi) < 2.1$ @ 90% C.L.
$\phi + K\bar{K}\pi$	$'f_1(1285)'$	$1279 \pm 6 \pm 10$	$14^{+20}_{-14} \pm 10$	$(J/\psi \to \phi' f_1(1285)') \cdot ('f_1(1285)' \to K\bar{K}\pi) = 0.6 \pm 0.2 \pm 0.1$
				$(J/\psi \to \gamma\varepsilon) \cdot (\varepsilon \to a_0(980)\pi) \cdot (a_0(980) \to \eta\pi)$
$\gamma + \eta\pi^+\pi^-$, $\eta \to \gamma\gamma$	$\eta(1275)$ or $f_1(1285)$	1283 fixed	26 fixed	$= 2.7 \pm 0.8 \pm 0.2$
$\gamma + \eta\pi^+\pi^-$, $\eta \to \pi^+\pi^-\pi^0$	ε?	1283 fixed	26 fixed	$= 3.2 \pm 1.1 \pm 0.3$
				$(J/\psi \to \gamma X) \cdot (X \to a_0(980)\pi) \cdot (a_0(980) \to \eta\pi)$
$\gamma + \eta\pi^+\pi^-$, $\eta \to \gamma\gamma$	X?	1382 ± 6	69 ± 23	$= 5.2 \pm 1.2 \pm 0.5$
$\gamma + \eta\pi^+\pi^-$, $\eta \to \pi^+\pi^-\pi^0$		1400 ± 7	62 ± 16	$= 5.2 \pm 1.8 \pm 0.5$
$\omega + \eta\pi^+\pi^-$	$'f_1(1420)'$?	$1421 \pm 8 \pm 10$	$45^{+32}_{-23} \pm 15$	$(J/\psi \to \omega' f_1(1420)') \cdot ('f_1(1420)' \to \eta\pi\pi) = 9.2 \pm 2.4 \pm 2.8$
$\phi + \eta\pi^+\pi^-$	$'\eta(1275)'$ or $'f_1(1285)'$?	$1283 \pm 6 \pm 10$	$24^{+20}_{-14} \pm 10$	$(J/\psi \to \phi\varepsilon) \cdot (\varepsilon \to \eta\pi\pi) = 1.6^{+0.6}_{-0.5} \pm 0.4$

† Results obtained from the initial 2.7×10^6 data sample.

$$J/\psi \to \phi \quad K^{\pm}K^0_S\pi^{\mp} \qquad ii)$$
$$\hookrightarrow K^+K^-$$
$$\to \phi \quad K^{\pm}K^0_S\pi^{\mp} \qquad iii)$$
$$\hookrightarrow K^0_L K^0_S$$

Figure 12(a), (b) show the reconstructed K^+K^- spectra from *i*) and *ii*) respectively, and Fig. 12 (c) shows the $K^0_L K^0_S$ spectrum from *iii*); a clean ϕ signal is apparent in all three plots. Figure 13 presents the combined $K\bar{K}\pi$ spectrum produced in association with a ϕ from *i*), *ii*) and *iii*). No clear structure is visible in the 1440 MeV/c^2 region. Apart from a small signal at 1280 MeV/c^2, the rest of the spectrum is dominated by a broad phase space like distribution.[54] The upper limits at a 90% C.L. for the $f_1(1420)$ and the $\eta(1440)$ production in association with the ϕ are quoted in Table 1. The inclusive branching ratios are also listed. The mass and the width of the structure at 1280 MeV/c^2 was measured to be

$$m = 1279 \pm 6 \pm 10 \quad \mathrm{MeV/c^2}$$
$$\Gamma = 14^{+20}_{-14} \pm 10 \quad \mathrm{MeV/c^2} \quad ,$$

consistent with those of the $f_1(1285)$ $\{D(1285)\}$, an isosinglet member of the 1^{++} nonet. Figure 14 shows the three $K\bar{K}\pi$ systems recoiling against a γ, an ω and a ϕ.

Neither the $f_1(1420)$ nor the $\eta(1440)$ is observed in the $K\bar{K}\pi$ mode recoiling against a ϕ. If the DOZI contributions could be neglected, this would strongly suggest that the $f_1(1420)$ does not have any substantial strange quark content. Furthermore, a structure consistent with the $f_1(1285)$, commonly believed to contain u, d quarks, is observed to be produced recoiling against a ϕ.

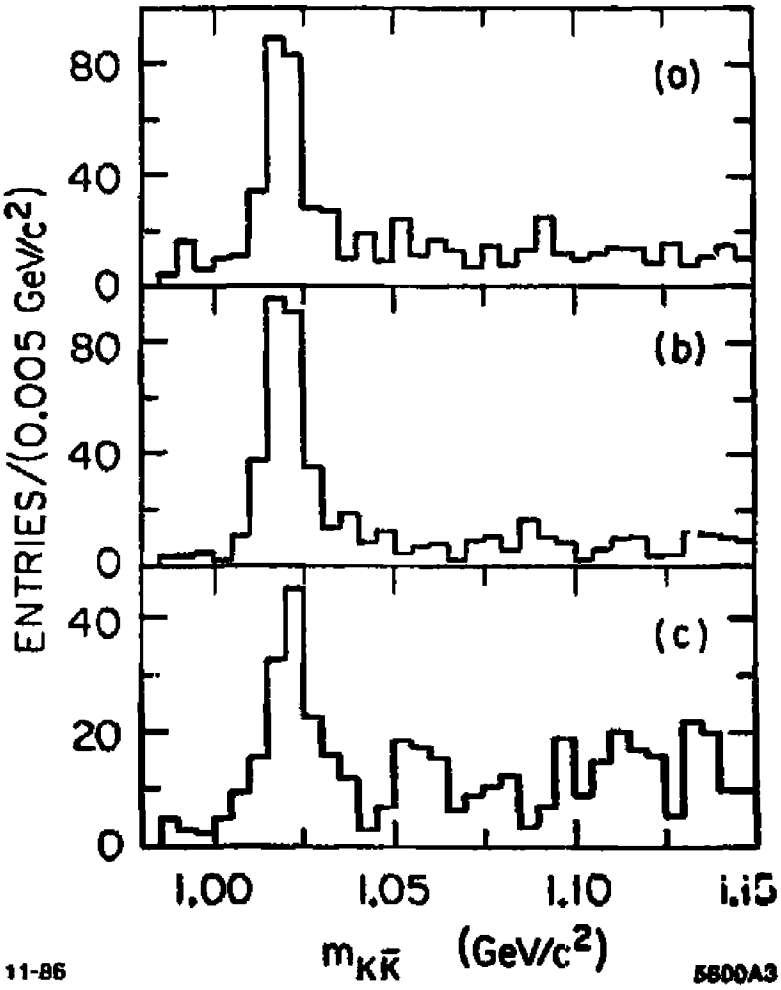

12. K^+K^- invariant mass distributions from (*a*) $J/\psi \to \phi K^+K^-\pi^0$ with four possible entries per event, (*b*) $J/\psi \to \phi K^\pm K_S^0\pi^\mp$ with two possible entries per event, and (*c*) $K_S^0K_L^0$ invariant mass distribution from $J/\psi \to \phi K^\pm K_S^0\pi^\mp$ with up to six entries per event. Background from events not containing K_S^0 is subtracted in (*b*) and (*c*).

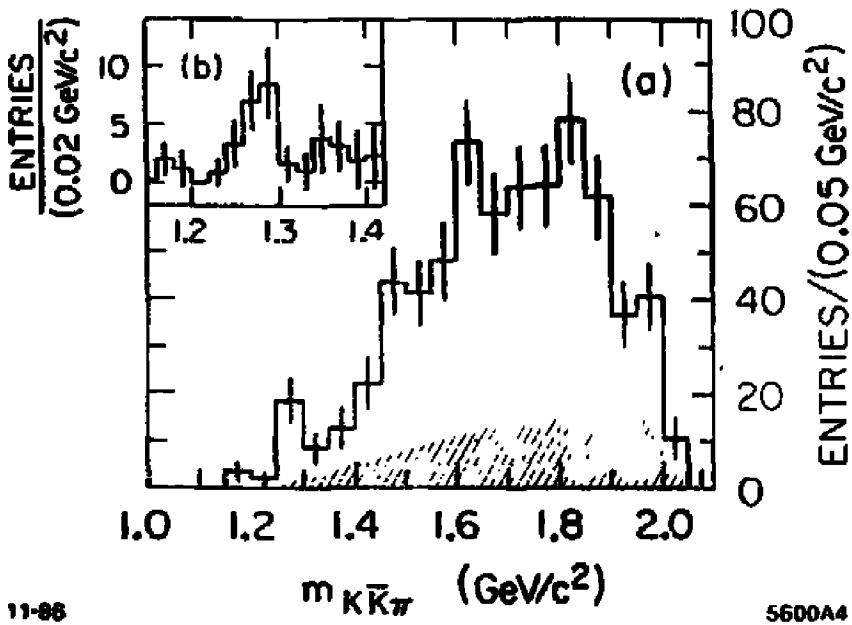

13. (a) Summed $K^+K^-\pi^0$ and $K^\pm K^0_S\pi^\mp$ invariant mass distributions from the reactions $J/\psi \to \phi K^+K^-\pi^0$ and $J/\psi \to \phi K^\pm K^0_S\pi^\mp$. The shaded area shows the estimate of the background. (b) Detail of 1200 MeV/c^2 mass region after selecting $m(K\bar{K})$ <1150 MeV/c^2 .

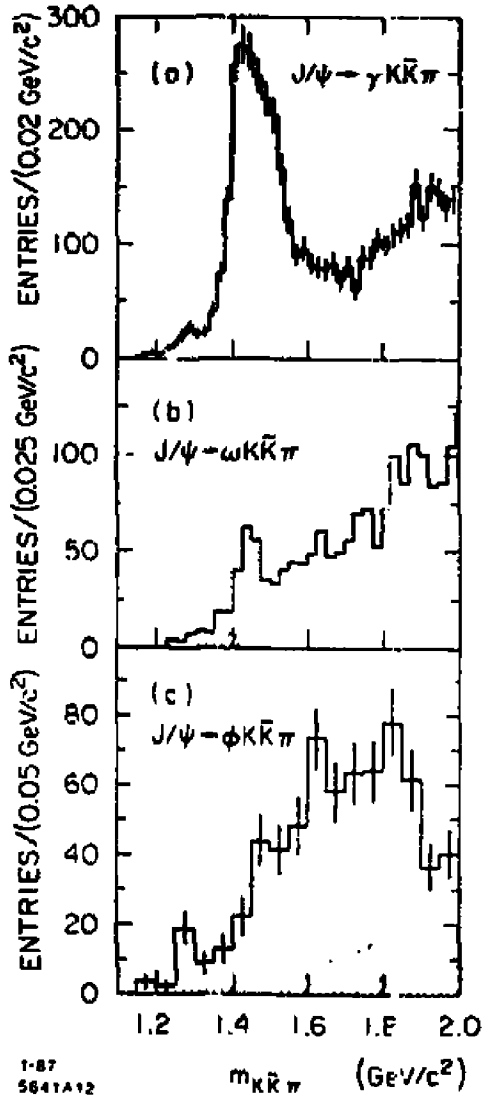

14. $K\bar{K}\pi$ mass spectra recoiling against (*a*) a γ, (*b*) and ω and (*c*) a ϕ. Shaded area represents the estimated background.

The $\eta\pi^+\pi^-$ Decay Mode

In the $K\bar{K}\pi$ system, an important question in identifying the resonance, has been isolating the isobaric intermediate state of its decay, namely, K^*K and $a_0(980)\pi$. The $a_0(980)$ has a large decay branching ratio into $\eta\pi$. Hence an ideal place to look for a solution to the $K\bar{K}\pi$ puzzle was in the $\eta\pi\pi$ system.

3.5 $J/\psi \rightarrow \gamma\eta\pi^+\pi^-$

The following two decay modes were observed,

$$J/\psi \rightarrow \eta\pi^+\pi^- + \gamma \quad \Big\lfloor \rightarrow \gamma\gamma \qquad \text{i)}$$

$$J/\psi \rightarrow \eta\pi^+\pi^- + \gamma \quad \Big\lfloor \rightarrow \pi^+\pi^-\pi^0 \qquad \text{ii)}$$

the invariant $\eta\pi^+\pi^-$ mass distributions from i) and from ii) are displayed in Fig. 15(a) and Fig. 15(b) respectively. A very sharp peak at $\sim$ 960 MeV/c^2 in both plots indicate copious $\eta'(958)$ production. Figure 16 (a),(b) show the $\eta\pi^\pm$ invariant mass spectra from i) and ii), in which copious $a_0(980)$ production is evident. The combined spectrum, with the $\eta\pi^+\pi^-$ invariant mass above 1000 MeV/c^2 is presented in Fig. 17(a), and shows many interesting structures. However, a sharp dip instead of a peak exists at the conventional mass of the $\eta(1440)$. Several possible explanations exist,[93] [96] one of these being that the dip is caused by destructive interference[93] between different decay modes of the $\eta(1440)$. Figure 17(b) depicts the $\eta\pi^+\pi^-$ spectrum where an intermediate $a_0(980)$ production was required. The 1200 $\sim$ 1600 MeV/c^2 region is thereby emphasized, and a narrow peak at $\sim$ 1280 MeV/c^2 and another narrow peak at $\sim$ 1390 MeV/c^2 are apparent. The exact mass and the width, assigned to the $\sim$ 1390 MeV/c^2 structure by a Breit-Wigner parametrization, are listed in Table 1. The respective branching ratios are also listed in Table 1.

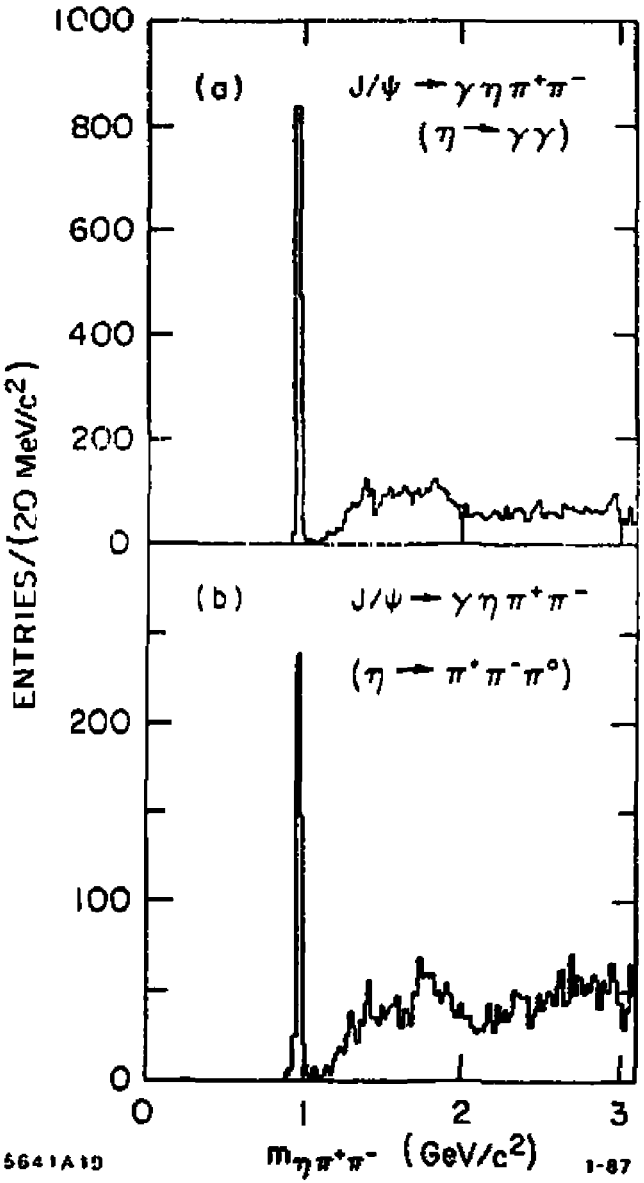

15. The $\eta\pi^+\pi^-$ mass spectra in the reaction $J/\psi \to \gamma\eta\pi^+\pi^-$ where the η decays into (*a*) $\gamma\gamma$ and (*b*) $\pi^+\pi^-\pi$.

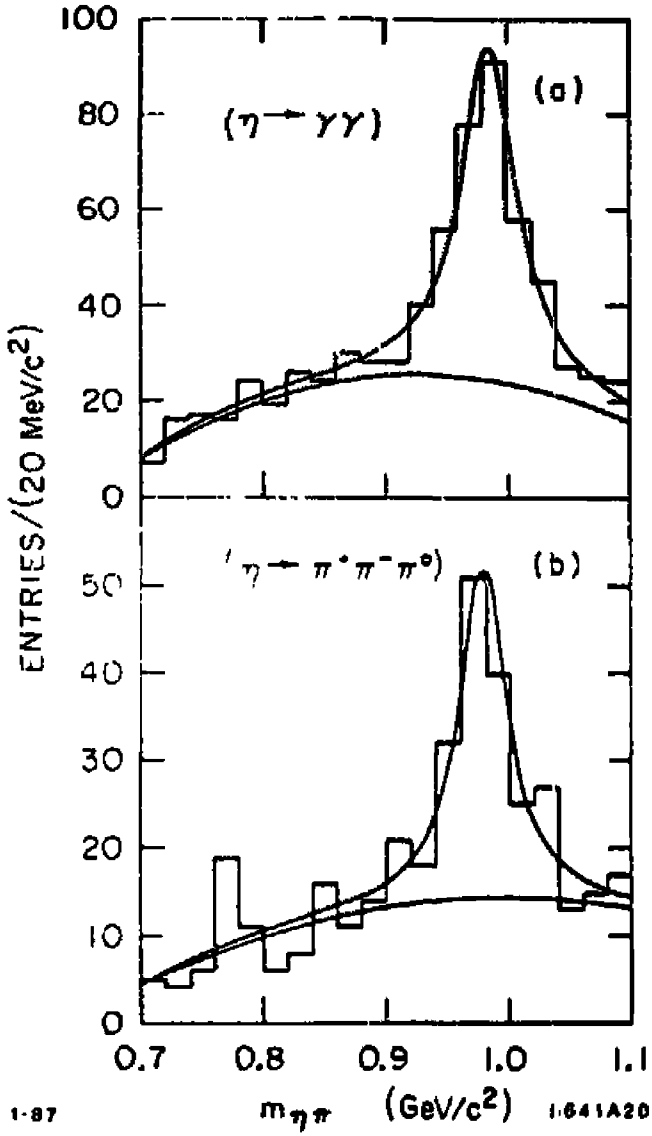

16. Example of $a_0(980)$ formation in the decay $J/\psi \rightarrow \gamma\eta\pi^+\pi^-$, e.g (*a*) in $\eta\pi^+$ where η decays into $\gamma\gamma$ and (*b*) in $\eta\pi^-$ where η decays into $\pi^+\pi^-\pi^0$.

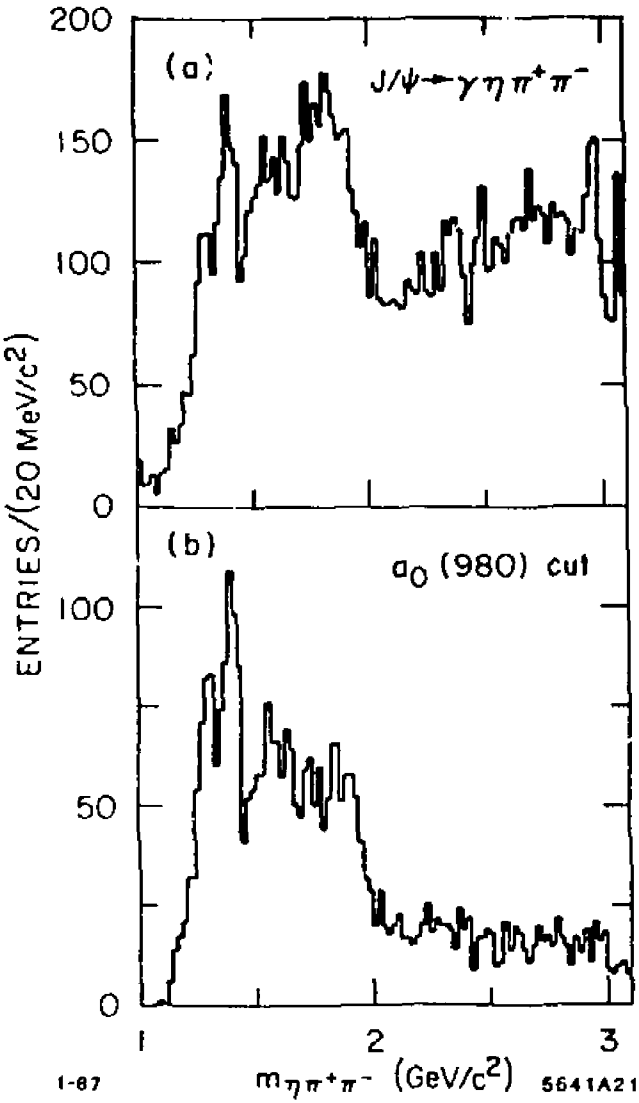

17. (*a*) $\eta\pi^+\pi^-$ effective mass spectrum where the two η decay modes are summed, (*b*) $\eta\pi^+\pi^-$ effective mass spectrum where an intermediate $a_0(930)$ formation is required.

The lower peak at 1285 MeV/c^2 is consistent with $f_1(1285)$, however it is also consistent with the $\eta(1275)$ reported[88] in the PWA of the $\eta\pi^+\pi^-$ system in fixed target experiments. The second peak occurs at a mass lower than the conventional $f_1(1420)$ mass. A complete PWA is required to clarify the situation. The mass region above 1500 MeV/c^2 is not discussed here, but shows interesting structures.

3.6 $J/\psi \to \omega\eta\pi^+\pi^-$

The following decay mode was investigated,

$$J/\psi \to \omega\,\eta \quad \pi^+\pi^-$$
$$\pi^+\pi^-\pi^0 \bullet\!\!\rightarrow \gamma\gamma.$$

Figure 18(a) presents the $\eta\pi^+\pi^-$ invariant mass spectrum recoiling against an ω. The $\eta'(958)$ is clearly visible along with a peak at the nominal $f_1(1285)$ and a peak at the $f_1(1420)$ mass. The masses and the widths were determined to be

$$m = 1283 \pm 6 \pm 10 \quad \mathrm{MeV}/c^2$$
$$\Gamma = 14^{+19}_{14} + 10 \quad \mathrm{MeV}/c^2$$

and

$$m = 1421 \pm 8 \pm 10 \quad \mathrm{MeV}/c^2$$
$$\Gamma = 45^{+32}_{-23} \pm 15 \quad \mathrm{MeV}/c^2 \ ,$$

respectively, for the 1285 MeV/c^2 and the 1420 MeV/c^2 peaks. The corresponding branching ratios are listed in Table 1.

A study of the substructure in $\eta\pi^+\pi^-$ yielded a significant amount of the $a_0(980)$ production. Figure 18(b) represents the $\eta\pi^+\pi^-$ invariant mass spectrum requiring that $\eta\pi$ system formed an $a_0(980)$. The $f_1(1285)$ region, seems consistent with all of the resonance proceeding through an intermediate state of $a_0(980)$, while in the $f_1(1420)$ region, the resonance proceeds dominantly through the $a_0(980)$. It is worth noting that the higher mass region in this $\eta\pi^+\pi^-$ spectrum in Fig. 18(a) seems very promising in terms of structures.

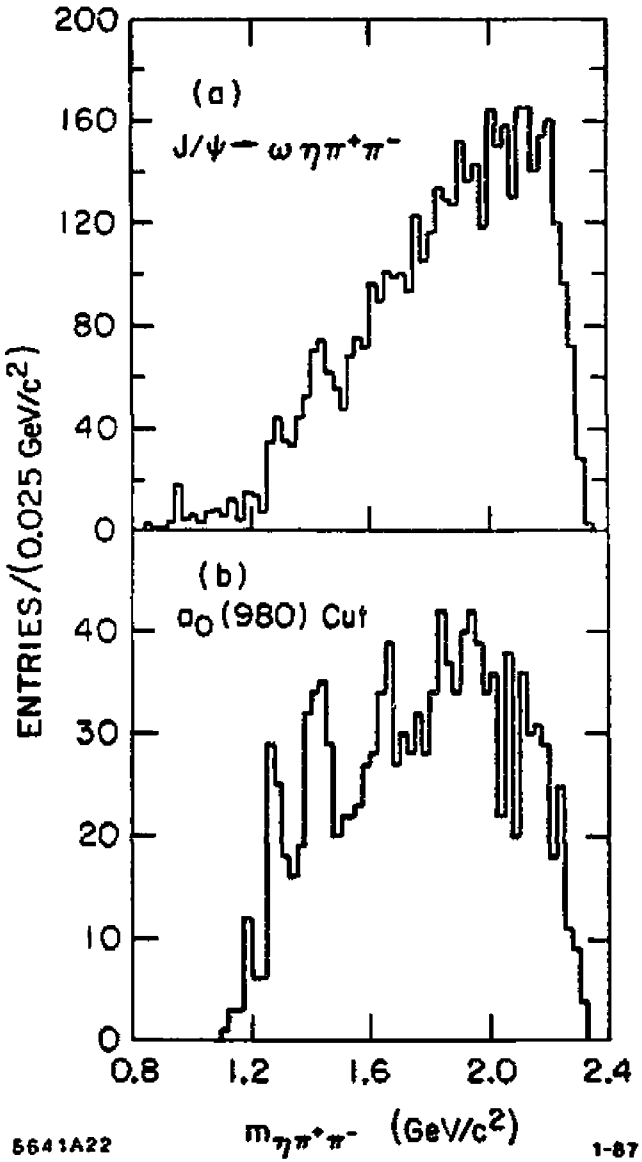

18. (*a*) $\eta\pi^+\pi^-$ invariant mass spectrum in the decay $J/\psi \rightarrow \omega\eta\pi^+\pi^-$, (*b*) $\eta\pi^+\pi^-$ invariant mass spectrum requiring an intermediate $a_0(980)$ formation.

3.7 $J/\psi \to \phi\eta\pi^+\pi^-$

The decay mode observed was,

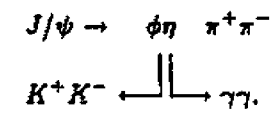

Figure 19 shows the invariant $\eta\pi^+\pi^-$ mass recoiling against the ϕ. A clean spectrum with a large $\eta'(958)$ signal is seen. At $\sim$ 1285 MeV/c^2 , a peak compatible with the $f_1(1285)$ is observed. The mass and the width as determined by a Breit-Wigner parametrization were,

$$m = 1283 \pm 6 \pm 10 \quad \text{MeV}/c^2$$
$$\Gamma = 24^{+20}_{-14} \pm 10 \quad \text{MeV}/c^2.$$

Again, similar to the spectrum of the $K\bar{K}\pi$ system recoiling against a ϕ, any production of the $\eta(1440)$ or the $f_1(1420)$ is not visible (a single high bin is observed). The relevant branching ratios are listed in Table 1. Similar to the previous decay modes, study of the substructure in the $\eta\pi^+\pi^-$ system revealed that the 1285 MeV/c^2 resonance decayed through an intermediate $a_0(980)$ state.

Figure 20 presents the $\eta\pi^+\pi^-$ spectrum recoiling against a γ, an ω and a ϕ. Figure 20(a) and (b) present the spectrum with the requirement of an $a_0(980)$ intermediate state. The conventional $\eta(1440)$ is not observed in the $\eta\pi\pi$ invariant mass spectrum in the radiative J/ψ decay. A narrow structure at $\sim$1400 MeV/c^2 is observed, along with an $f_1(1285)$-like structure at the appropriate mass. In the hadronic decay of the J/ψ, an $f_1(1285)$-like and an $f_1(1420)$-like structure are seen to be produced in association with an ω, while only an $f_1(1285)$ like structure is seen to be produced in association with a ϕ.

To recapitulate, at the time the $\eta(1440)$ was first observed, the $f_1(1420)$ was established as the $s\bar{s}$ member and the $f_1(1285)$ as the $(u\bar{u} + d\bar{d})$ member of the 1^{++} family. These interpretations stemmed from the mass formula[37]

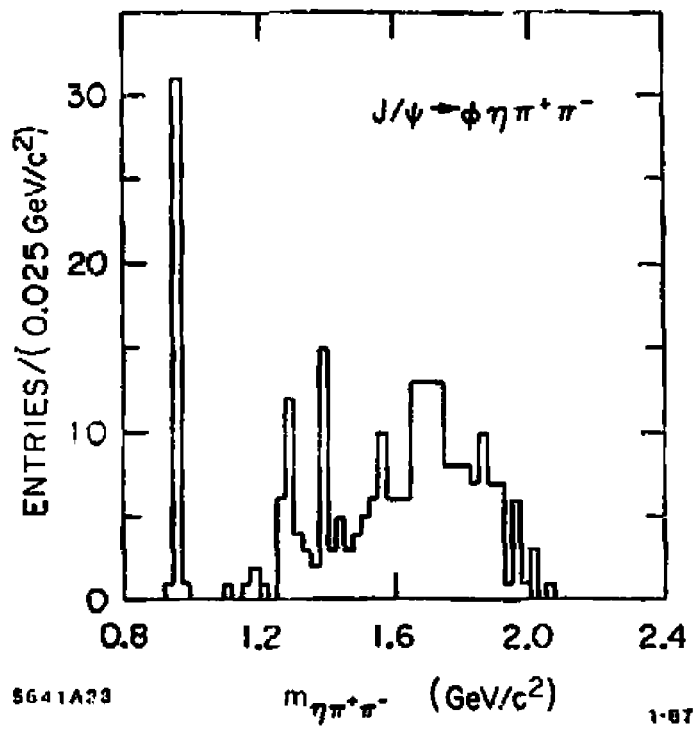

19. The $\eta\pi^+\pi^-$ invariant mass spectrum in the decay $J/\psi \to \phi\eta\,\pi^+\pi^-$.

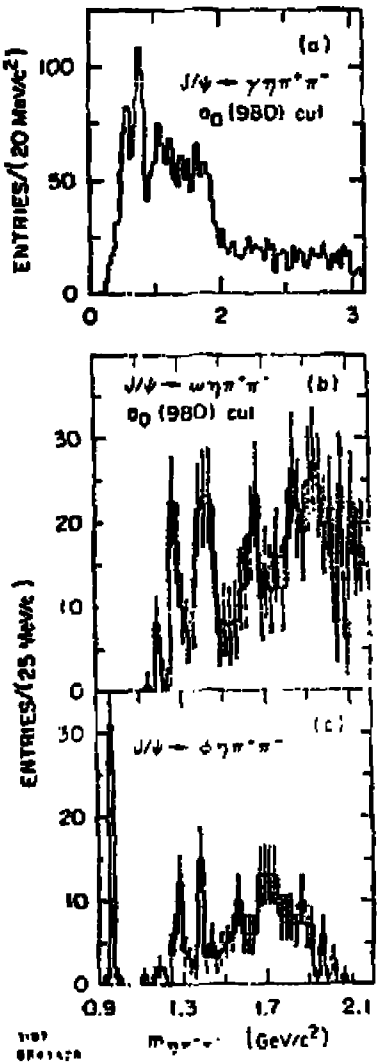

20. The $\eta\pi^+\pi^-$ (background subtracted) invariant mass spectra from the reactions (a) $J/\psi \to \gamma\eta\pi^+\pi^-$, (b) $J/\psi \to \omega\eta\pi^+\pi^-$ and (c) $J/\psi \to \phi\pi^+\pi^-$.

$$m_{a_1(1270)} = m_{f_1(1285)}$$

$$2m_{Q_A(1340)} = m_{f_1(1285)} + m_{f_1(1420)}$$

and from the fact that the $f_1(1420)$ was observed to decay into $K\bar{K}\pi$, while the $f_1(1285)$ decayed primarily into $\eta\pi\pi$. Recently, as discussed earlier, the $\eta(1440)$ is established as a 0^-, and the identity of the $f_1(1440)$ as an axial vector or a pseudoscalar state as well as an $s\bar{s}$ state has been seriously questioned. Several questions are raised by the MARK III data which need to be answered, e.g. whether the peaks seen in $K\bar{K}\pi$ and in $\eta\pi\pi$ (consistent with the $f_1(1420)$) recoiling against an ω are the same objects, and whether the peak in $\eta\pi\pi$ in the radiative decay is the same. Curiously, in the recoil against the ϕ, no peak is observed at the $f_1(1420)/\eta(1440)$ mass region. Several explanations have been attempted[138] [139] to accommodate all the data in this region from the J/ψ decay, fixed target reactions and the radiative and the two photon width measurements. One of these[88] suggests that the $K\bar{K}\pi$ peak observed in association with an ω in the J/ψ decay as well as that observed in the 2-γ reaction[82] is a hybrid $q\bar{q}g$ 1^{-+} exotic state, and the state observed in $\eta\pi\pi$ in association with an ω is a different state.

The 1280 MeV/c^2 region is somewhat complicated because of the presence of the $\eta(1275)$ (the radial excitation of the η), in addition to the $f_1(1285)$. Assuming that MARK III data shows the $f_1(1285)$ in $\eta\pi\pi$ in associated production with ϕ and ω in the J/ψ decay, it casts doubt on the pure $(u\bar{u} + d\bar{d})$ interpretation of the $f_1(1285)$, if DOZI correlations were to be ignored.

4. In Search of the $f_2(1720)$

As discussed earlier, it will be a triumph for QCD if a strongly interacting gluonic bound state or a hybrid state, namely a bound state of quarks and gluons is observed. Identifying such a state will be an experimental success. The $f_2(1720)$ has been a prime candidate for such a state. It was first observed[3] in radiative J/ψ decay, $J/\psi \to \gamma\eta\eta$. MARK III observed[17] the $f_2(1720)$ in radiative decay in $K\bar{K}$ and $\pi^+\pi^-$, in its initial 2.7×10^6 data sample. The measured branching ratio into K^+K^- was,

$$B(J/\psi \to \gamma f_2(1720)) \cdot (f_2(1720) \to K^+K^-) = (4.8 \pm 0.6 \pm 0.9) \times 10^{-4}.$$

The mass and the width were

$$m = 1720 \pm 7 \quad \text{MeV/c}^2$$
$$\Gamma = 132 \pm 15 \quad \text{MeV/c}^2.$$

The spin parity was determined to be 2^+. Figure 3(a) and 3(b) show the K^+K^- and $K^0_SK^0_S$ invariant mass spectra from the updated data sample in the reactions $J/\psi \to \gamma K^+K^-$ and $J/\psi \to \gamma K^0_SK^0_S$, respectively. A clear $f_2(1720)$ is seen in both plots, along with the $f_2'(1525)$. In the $K^0_SK^0_S$ mode, a maximum likelihood fit to the helicity amplitudes[18] yielded $J^P = 2^+$ for both the $f_2'(1525)$ and the $f_2(1720)$. Observation of the $f_2(1720)$ in the decay mode $J/\psi \to \gamma\pi^+\pi^-$ was also reported[17] by MARK III. The mass and the width of the $f_2(1720)$ from this decay mode were measured to be

$$m = 1713 \pm 15 \quad \text{MeV/c}^2$$
$$\Gamma = 130 \quad \text{MeV/c}^2\text{(fixed)}.$$

The branching ratio was measured as

$$B(J/\psi \to \gamma f_2(1720)) \cdot (f_2(1720) \to \pi^+\pi^-) = (1.6 \pm 0.4 \pm 0.3) \times 10^{-4}.$$

Figure 21(a) shows the invariant $\pi^+\pi^-$ mass spectrum from the complete data sample. The low mass peak at ~700 MeV/c^2 is feed-through events from the

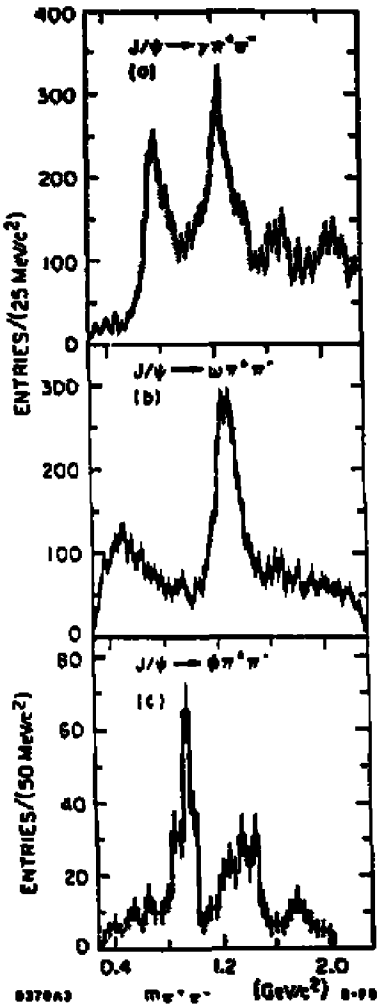

21. The $\pi^+\pi^-$ effective mass spectra in the reactions (a) $J/\psi \to \gamma\pi^+\pi^-$, (b) $J/\psi \to \omega\pi^+\pi^-$, and (c) $J/\psi \to \phi\pi^+\pi^-$.

$J/\psi \to \rho^0\pi^0$ decay mode, where one photon has not been detected. The $f_2(1270)$ $\{f(1270)\}$ is observed along with a shoulder possibly due to the $f_2'(1525)$ production. The $f_2(1720)$ is clearly observed at the expected mass. A structure is seen at ~2100 MeV/c^2 . This was previously reported[177] as possible evidence of production of the $f_4(2030)$ $\{h(2030)\}$. A detailed analysis is underway. An analysis of the radiative decay mode $J/\psi \to \gamma\eta\eta$ is also in progress.

Hadronic Searches

4.1 ωK^+K^- AND ϕK^+K^-

The comparison of a state produced in the radiative decay mode and a similar state produced in hadronic decay modes proved to be a useful tool to differentiate between the 'glue' and the quark content of the state, as described earlier. The same technique was employed to understand the nature of the $f_2(1720)$. Figure 22 displays the three K^+K^- spectra.

Figure 22(b) displays the K^+K^- effective mass spectrum observed in association with an ω in the reaction

$$J/\psi \to \omega + K^+K^-$$
$$\qquad\quad \hookrightarrow \pi^+\pi^-\pi^0.$$

An $f_2(1720)$-like peak is observed with a mass and a width of

$$m = 1731 \pm 10 \pm 10 \quad \text{MeV}/c^2$$
$$\Gamma = 110^{+45}_{-35} \pm 15 \quad \text{MeV}/c^2.$$

These parameters are consistent with those of the $f_2(1720)$. The measured branching ratio was

$$B(J/\psi \to \omega' f_2(1720)') \cdot (' f_2(1720)' \to K\bar{K}) = (4.5^{+1.2}_{-1.1} \pm 1.0) \times 10^{-4}.$$

The $K^0_S K^0_S$ mode yields consistent results, although with smaller statistics.

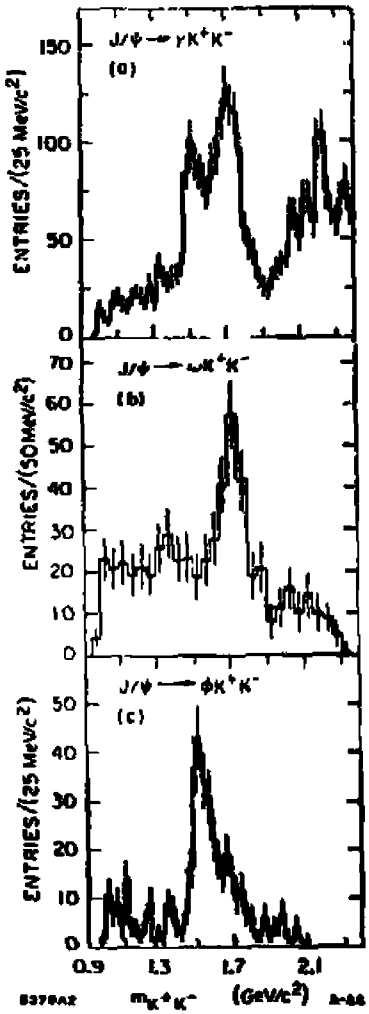

22. The K^+K^- effective mass spectra in the reactions (a) $J/\psi \to \gamma K^+K^-$, (b) $J/\psi \to \omega K^+K^-$, and (c) $J/\psi \to \phi K^+K^-$.

Figure 22(c) shows the K^+K^- spectrum recoiling against a ϕ in the decay mode,

$$J/\psi \rightarrow \phi \quad K^+K^-$$
$$\qquad\qquad \hookrightarrow K^+K^-.$$

A prominent $f_2'(1525)$ is observed, with a clear shoulder on the high mass side. A coherent fit with standard $f_2(1720)$ parameters describe the data very well. A detailed study with the proper mix of the angular distributions is underway.

4.2 $\omega\pi^+\pi^-$ AND $\phi\pi^+\pi^-$

The radiative $\pi^+\pi^-$ spectrum was compared with the $\pi^+\pi^-$ spectra in hadronic decays, produced in association with a ϕ and an ω, as shown in Figure 21. Figure 21(b) displays the $\pi^+\pi^-$ spectrum from the decay mode,

$$J/\psi \rightarrow \omega \quad \pi^+\pi^-$$
$$\qquad\qquad \hookrightarrow \pi^+\pi^-\pi^0.$$

As expected from the quark correlations, a clear $f_2(1270)$ is observed. No obvious structure at the $f_2(1720)$ is seen. The $\pi^+\pi^-$ spectrum is described later in some detail. Figure 21(c) presents the $\pi^+\pi^-$ spectrum from the decay mode,

$$J/\psi \rightarrow \phi\, \pi^+\pi^-$$
$$\qquad\qquad \hookrightarrow K^+K^-.$$

A clear $f_0(975)\{S(975)\}$ and a broad structure in the 1400-1500 MeV/c^2 are observed and will be discussed later. A structure, similar in mass and width of those of the $f_2(1720)$, is observed.

In summary, the $f_2(1720)$ has been observed in the radiative decays of the J/ψ into K^+K^-, $K_S^0K_S^0$ and $\pi^+\pi^-$, with large branching ratios. The analysis of the radiative decay mode, $J/\psi \rightarrow \gamma\eta\eta$ is in progress. Comparisons with the

hadronic channels yield interesting results. An $f_2(1720)$-like structure is observed in $K\bar{K}$ produced in association with an ω, and in $\pi^+\pi^-$ produced in association with a ϕ, where the conventional $q\bar{q}$ mesons are not expected to be produced profusely. In $K\bar{K}$, in association with a ϕ, the $f_2(1720)$-like structure is seen as only a shoulder to the $f_2'(1525)$, although a detailed analysis will yield more definitive results.

5. Quark Correlations

The study of quark correlations can be extended to whole meson nonets, namely the members of any nonet recoiling against members of the vector nonet. The vector nonet was chosen because it is ideally mixed. The nonet correlations investigated so far are,

$$\begin{aligned} J/\psi \rightarrow\ & \text{Vector} + \text{Pseudoscalar} \\ & + \text{Tensor} \\ & + \text{Scalar} \end{aligned}$$

All the Vector-Pseudoscalar decay branching ratios were measured[39] from the previous data sample. By observing and measuring the decays

$$\begin{aligned} J/\psi &\rightarrow \omega\eta \\ &\rightarrow \phi\eta \end{aligned}$$

and

$$\begin{aligned} J/\psi &\rightarrow \omega\eta' \\ &\rightarrow \phi\eta' \end{aligned}$$

the quark contents of the η and the η' were determined.[40] From measuring all the decay modes, shown in Table 2, the strong, the electromagnetic and the SU(3) violating amplitudes were determined.

A similar study is almost completed for the Vector-Tensor case, and has begun for the Vector-Scalar.

TABLE 2. $J/\psi \rightarrow$ V-P Decay Amplitudes[40],[47]

Decay mode	Amplitude	Amplitude with DOZI
$\rho^+\pi^-, \rho^0\pi^0\rho^-\pi^+$	$g+e$	$g+e$
$K^{*+}K^-, K^{*-}K^+$	$g-h+e(2-x)$	$g-h+e(2-x)$
$K^{*0}\bar{K}^0, \bar{K}^{*0}K^0$	$g-h-2e(\frac{1+x}{2})$	$g-h-2e(\frac{1+x}{2})$
$\omega\eta$	$(g+e)\chi_\eta$	$(g+e)\chi_\eta + \sqrt{2}\,\gamma g(\sqrt{2}\chi_\eta + Y_\eta)$
$\omega\eta'$	$(g+e)\chi_{\eta'}$	$(g+e)\chi_{\eta'} + \sqrt{2}\,\gamma g(\sqrt{2}\chi_{\eta'} + Y_\eta)$
$\phi\eta$	$(g-2h-2ex)Y_\eta$	$(g-2h-2ex)Y_\eta + \gamma(g-h)\,(\sqrt{2}\chi_\eta + Y_\eta)$
$\phi\eta'$	$(g-2h-2ex)Y'_\eta$	$(g-2h-2ex)Y_{\eta'} + \gamma\,(g-h)(\sqrt{2}\chi_{\eta'} + Y_{\eta'})$
$\rho^0\eta$	$3e\chi_\eta$	$3e\chi_\eta$
$\rho^0\eta'$	$3e\chi_{\eta'}$	$3e\chi_{\eta'}$
$\omega\pi^0$	$3e$	$3e$
$\Phi\pi^0$	0	0

$X_\eta \rightarrow \sqrt{2}(u\bar{u} + d\bar{d}$ *content of* η, $Y_\eta \rightarrow s\bar{s}$ *content of* η,

$X'_\eta \rightarrow \sqrt{2}(u\bar{u} + d\bar{d})$ *content of* η', $Y'_\eta \rightarrow s\bar{s}$ *content of* η',

$g \rightarrow SU(3)$ *symmetric strong amplitude*, $e \rightarrow$ *electromagnetic amplitude*,

$h \rightarrow SU(3)$ *violating amplitude*, $x \rightarrow$ *ratio of s and u quark magnetic moments*,

$r \rightarrow$ *ratio of DOZI and strong amplitudes.*

5.1 THE I=0 CORRELATION

$J/\psi \to \phi\pi^+\pi^-$

Figure 21(c) shows the $\pi^+\pi^-$ spectrum recoiling against a ϕ. As mentioned earlier, the $f_0(975)$ is observed in its characteristic asymmetric way. The $f_0(975)$, in the $q\bar{q}$ scheme is an $I = 0$, $s\bar{s}$ member of the 0^{++} nonet. Several other interpretations of $f_0(975)$ exist, including a $qq\bar{q}\bar{q}$[41] or a molecule,[42] and as two states close to each other, one an $s\bar{s}$ meson and the other, a glueball candidate[43] (a pole in $\pi\pi$ and another in $K\bar{K}$). In the $s\bar{s}$ scheme, the $f_0(975)$ would prefer to decay into $K\bar{K}$, but, being below $K\bar{K}$ threshold, decays mostly into $\pi\pi$. However, once the invariant mass is above the $K\bar{K}$ threshold, it decays mostly to $K\bar{K}$ and hence the sharp fall-off in $\pi\pi$ on the high mass side of the $f_0(975)$. The branching ratio was measured using the standard coupled channel Flatté parametrization[44] (which is an approximation, a simple extension of a formulation for non-relativistic systems) and also using a more exact formalism which is relativistic. The same branching ratio was obtained with both parametrizations,

$$B \cdot (J/\psi \to \phi f_0(975)) \cdot (f_0(975) \to \pi^+\pi^-) = (2.3 \pm 0.3 \pm 0.6) \times 10^{-4}.$$

In the 1300 - 1500 MeV/c^2 mass region, one or more structures are visible. There are simply speculations regarding their identities, because of limited statistics. One might attribute these structures to the $f_2(1270)$ and the $f_0(1300)\{\epsilon(1300)\}$. The structure at $\sim$ 1750 MeV/c^2 has been discussed previously.

$J/\psi \to \phi K^+K^-$

Figure 22(c) shows the K^+K^- spectrum recoiling against a ϕ. A clear $f_2'(1525)$ is observed. This is expected from the quark correlations, since the 2^{++} nonet is almost ideally mixed and $f_2'(1525)$ contains $s\bar{s}$. As mentioned earlier, a shoulder possibly due to the $f_2(1720)$ production is present. The branching ratio derived for $f_2'(1525)$ production does not depend substantially on the '$f_2(1720)$'

parametrization. The measured branching ratio is

$$B \cdot (J/\psi \to \phi f'(1525)) \cdot (f'(1525) \to K\bar{K}) = (6.4 \pm 0.6 \pm 1.6) \times 10^{-4},$$

where the mass and the width of the $f_2'(1525)$ were fixed at

$$\begin{aligned} m &= 1520 \quad \mathrm{MeV/c^2} \\ \Gamma &= 75 \quad \mathrm{MeV/c^2}. \end{aligned}$$

$J/\psi \to \omega\pi^+\pi^-$

Figure 21(b) presents the $\pi^+\pi^-$ spectrum recoiling against an ω in the decay

$$J/\psi \to \omega \quad \pi^+\pi^- \\ \qquad\quad \lfloor\!\_ \; \pi^+\pi^-\pi^0.$$

The $f_2(1270)$ is very pronounced. The branching ratio was measured as

$$B \cdot (J/\psi \to \omega f_2(1270)) \cdot (f_2(1270) \to \pi^+\pi^-) = (27.7 \pm 1.4 \pm 7.0) \times 10^{-4}.$$

The lower mass region features a broad enchancement at ~500 MeV/c^2 which was seen in previous experiments. Several speculations exist as to the nature of it. The angular distributions of the ω (recoiling against this structure) in its helicity frame behaves like $\sin^2\theta$, consistent with the ω being aligned and the low mass structure having spin 0.

There is a small structure at ~970 MeV/c^2 consistent with some $f_0(975)$ production, with a branching ratio $\sim 10^{-4}$ from simple event counts.

$J/\psi \to \omega K\bar{K}$

As discussed earlier, Fig. 22(b) displays the K^+K^- spectrum from the decay mode,

$$J/\psi \to \omega \quad K^+K^-$$
$$\qquad\qquad \hookrightarrow \pi^+\pi^-\pi^0.$$

None of the conventional $q\bar{q}$ type mesons are seemingly observed. An upper limit for $f_2'(1525)$ production is measured as

$$B \cdot (J/\psi \to \omega f_2'(1525)) \cdot (f_2'(1525) \to K\bar{K}) < 1.2 \times 10^{-4} \quad \text{at 90\% C.L.}$$

The $K_S^0K_S^0$ channel, although lower in statistics, shows similar features.

5.2 The $I = 1/2$ Correlation

The following decay mode was observed

$$J/\psi \to \quad K^*(892)^0\ \overline{K^*_2(1430)}^0 \ + \ cc.$$
$$K^+\pi^- \hookleftarrow \qquad\qquad \hookrightarrow K^-\pi^+$$

Figure 23(a) shows the plot of $K^-\pi^+$ vs $K^+\pi^-$ effective mass. A band due to $K^*(892)$ (or cc) production is observed. Figure 23(b) shows the $K^-\pi^+$ spectrum recoiling against the $K^*(892)$. A very large peak at the $\overline{K^*_2(1430)}^0$ is evident. The production branching ratio was measured as

$$B \cdot (J/\psi \to K^*(892)^0\ \overline{K^*_2(1430)}^0) \ + \ cc = (120 \pm 20 \pm 22) \times 10^{-4}.$$

There is a hint of a shoulder on the low mass side of the $\overline{K^*_2(1430)}^0$. The $I = 1/2$ member of the 0^{++} family, the $K^{*0}(1350)$ $\{\kappa(1350)\}$ is reported to be $\sim$1350 MeV/c^2 with a width of $\sim$250 MeV/c^2 . However, it has so far been observed only in PWA. Hence, further analysis is needed to clarify the $K^{*0}(1350)$.

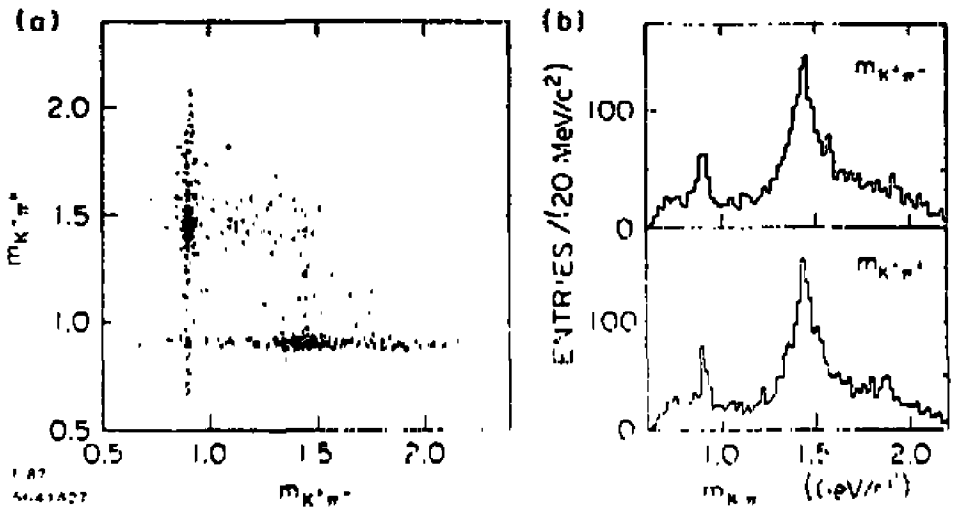

23. (*a*) **Scatter plot of** $K^-\pi^+$ **vs** $K^+\pi^-$ **effective mass in the reaction** $J/\psi \to$ $K^{*0}(892)\,\overline{K^{*0}(1430)}^0$ + *cc.* (*b*) **The** $K^-\pi^+$ **and** $K^+\pi^-$ **projections.**

5.3 THE $I = 1$ CORRELATION

The associated production with a ρ was observed in the following decay mode,

$$J/\psi \rightarrow \rho a_2(1320)$$
$$\pi\pi \leftarrow\!\!\rfloor\!\!\lfloor \rightarrow \eta\pi\pi$$

in all three charged states, namely $\rho^{\pm}a_2^{\mp}(1320)$ and $\rho^0 a_2^0(1320)$. The final state observed was $\eta\pi^+\pi^-\pi^0$. (The $\rho^{\pm}(\rho^0)$ decays into $\pi^0\pi^{\pm}(\pi^+\pi^-)$ and the $a_2^{\mp}(1320)$ $(a_2^0(1320))$ decays into $\eta\pi^{\mp}(\eta\pi^0)$.)

The same final state also yielded information about the reaction

$$J/\psi \rightarrow \rho a_0(980)$$
$$\pi\pi \leftarrow\!\!\rfloor\!\!\lfloor \rightarrow \eta\pi\pi$$

in all three charged states i.e. $\rho^{\pm}a_0^{\mp}(980)$ and $\rho^0 a_0^0(980)$.

Figure 24 displays the combined spectra of $\eta\pi^-$, $\eta\pi^0$, and $\eta\pi^+$, recoiling against a ρ^+, ρ^0, and ρ^-, respectively. A peak from the $a_2(1320)$ production over a smooth background is apparent. However, no obvious signal for the $a_0(980)$, correlated with the ρ production is seen. The branching ratio for $\rho a_2(1320)$ is measured as

$$B \cdot (J/\psi \rightarrow \rho\, a_2(1320)) = (118 \pm 8 \pm 29) \times 10^{-4}$$

An upper limit for the $\rho\, a_0(980)$ production was obtained as

$$B \cdot (J/\psi \rightarrow \rho\, a_0(980)) \cdot (a_0(980) \rightarrow \eta\pi) < 4.4 \times 10^{-4} \text{ at } 90\% \text{ C.L.}$$

Table 3 lists some of the relevant branching ratios. The quark correlations seem to exist, at least qualitatively. The branching ratios for the associated productions

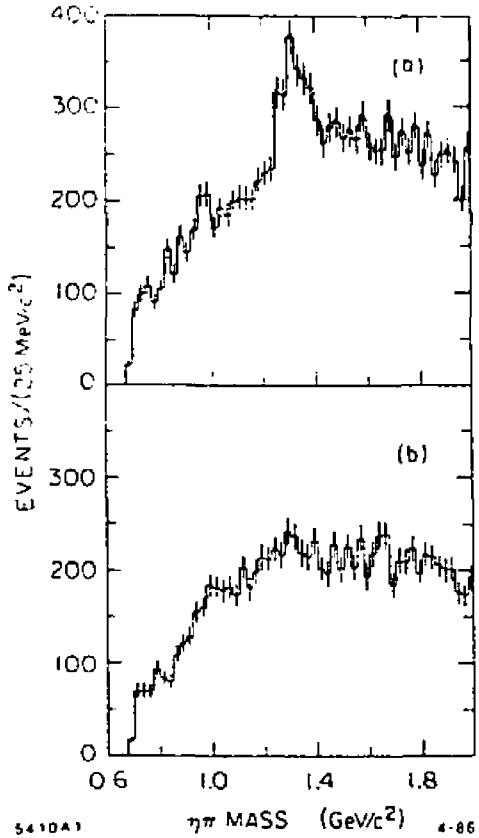

24. (*a*) Sum of $\eta\pi^+, \eta\pi^-$, and $\eta\pi^0$ mass spectra recoiling against a ρ in the reactions $J/\psi \to \rho\, a_2(1320)$ and $\rho\, a_0(980)$ where $a_2(1320)$ and $a_0(980)$ decay into $\eta\pi$ (all three charged states). (*b*) Sum of $\eta\pi^+$, $\eta\pi^-$, and $\eta\pi^0$ associated with ρ sidebands.

TABLE 3. Measured Branching Ratios into K^+K^- and $\pi^+\pi^-$

Decay mode $J/\psi \to$	Object	Mass MeV/c^2	Width MeV/c^2	Branching Ratio $\times 10^{-4}$
† $\gamma + K^+K^-$	$f_2'(1525)$	$1525 \pm 10 \pm 10$	85 ± 35	$(J/\psi \to \gamma f'(1525)) \cdot (f_2'(1525) \to K^+K^-) = 3.0 \pm 0.7 \pm 0.6$
† $\gamma + K^+K^-$	$f_2(1720)$	$1720 \pm 10 \pm 10$	130 ± 20	$(J/\psi \to \gamma f_2(1720)) \cdot (f_2(1720) \to K^+K^-) = 4.8 \pm 0.6 \pm 0.9$
$\omega + K^+K^-$	$f_2'(1525)$	1520 fixed	75 fixed	$(J/\psi \to \omega f_2'(1525)) \cdot (f_2'(1525) \to K\bar{K}) < 1.2$ @ 90% C.L.
$\omega + K^+K^-$	$f_2(1720)$?	$1731 \pm 10 \pm 10$	$110^{+46}_{-35} \pm 15$	$(J/\psi \to \omega' f_2(1720)') \cdot (f_2(1720)' \to K\bar{K}) = 4.5^{+1.3}_{-1.1} \pm 1.6$
$\phi + K^+K^-$	$f_2'(1525)$	1520 fixed	75 fixed	$(J/\psi \to \phi f_2'(1525)) \cdot (f_2'(1525) \to K\bar{K}) = 6.4 \pm 0.6 \pm 1.6$
† $\gamma + \pi^+\pi^-$	$f_2(1720)$	1713 ± 5	130 fixed	$(J/\psi \to \gamma f_2(1720)) \cdot (f_2(1720) \to \pi^+\pi^-) = 1.6 \pm 0.4 \pm 0.3$
† $\gamma + \pi^+\pi^-$	$f_2(1270)$	1269 ± 13	180 fixed	$(J/\psi \to \gamma f_2(1270)) \cdot (f_2(1270) \to \pi^+\pi^-) = 11.5 \pm 0.7 \pm 1.9$
† $\gamma + \pi^+\pi^-$	$f_0(975)$	975 fixed	35 fixed	$(J/\psi \to \gamma f_0(975)) \cdot (f_0(975) \to \pi\pi) =< 0.7$ @ 90% C.L.
$\omega + \pi^+\pi^-$	$f_2(1270)$	1277 fixed	182 ± 10	$(J/\psi \to \omega f_2(1270)) \cdot (f_2(1270) \to \pi^+\pi^-) = 27.7 \pm 1.4 \pm 7.0$
$\phi + \pi^+\pi^-$	$f_0(975)$	coupled channel	coupled channel	$(J/\psi \to \phi f_0(975)) \cdot (f_0(975) \to \pi^+\pi^-) = 2.3 \pm 0.3 \pm 0.8$

† Results obtained from the initial 2.7×10^6 data sample.

of $\omega f_2(1270)$, $\phi f_2'(1525)$, K*(892) $\overline{\mathrm{K}^*{}_2(1430)}$ + cc, and $\rho a_2(1320)$ in J/ψ decays are large, while $\omega f_2'(1525)$ and $\phi f_2(1720)$ are not. However, there is a striking difference between the branching ratios into the $\phi f_2'(1525)$ and $\omega f_2(1270)$ modes even after considering the effects of phase-space. The question of SU(3) violation is important. The question of how rigorous the quark correlations are, i.e. to what extent the DOZI processes are significant, is discussed later.

A systematic study of the scalars has started as is evident from Table 3. Perhaps most importantly, it could yield the answer to the question as to the nature of the scalars. The lack of observation of $\rho a_0(980)$ production raises questions about the $q\bar{q}$ interpretation of the $a_0(980)$, according to which the wavefunction of the $a_0(980)$ is

$$| a_0(980) >= \frac{1}{\sqrt{2}} | u\bar{u} - d\bar{d} > .$$

This is to be compared with similar associated production branching ratios of $\rho a_2(1320)$ and $\rho\pi$,[40] ($\sim 100 \times 10^{-4}$), where both the $a_2(1320)$ and π are well established $q\bar{q}$ mesons ($|\rho >= \frac{1}{\sqrt{2}} | u\bar{u} - d\bar{d} >$, $|\pi >= \frac{1}{\sqrt{2}} |u\bar{u} - d\bar{d} >$).

Several explanations,[41][42] including a molecule interpretation of the $a_0(980)$ relating to the 2γ-width[43] exist.

6. The DOZI Interpretation

Table 2 lists the Vector-Pseudoscalar decay modes expressed in terms of the strong, the electromagnetic and the SU(3) violating amplitudes. The SU(3) violation is present in both the strong and the electromagnetic amplitudes. The mixing angle of the Pseudoscalar nonet, (alternatively, the quark contents of the η and the $\eta'(958)$) were determined[40] by fitting these amplitudes to the data.‡

However, the recent measurement of the two photon width[16] of the $\eta'(958)$

‡ The η contained only u, d, and s quarks, while the $\eta'(958)$ had room for something extra.

disagreed with this conclusion and was consistent with it containing only u, d, and s quark as well.

Following the suggestions[46] [47] that the DOZI amplitude may be small but not negligible, and assuming that DOZI amplitude = $r \times$ strong amplitude, one can replace the previous expressions with[47] the new ones shown also in Table 2. It should be noted that the isospin conservation is still respected by the DOZI process. Currently, some of the Vector-Pseudoscalar decay modes are being updated with the present data sample and a refit of the amplitudes shown in Table 2 with the DOZI is in progress.

7. Conclusion

The baryonic decays are not discussed in the present paper, but a complete analysis is being pursued.

Interesting structures were observed[43] [48] [50] [38] in $\rho\rho$,[43] $\omega\omega$,[49] and $\gamma\rho$[39] in radiative decays of the J/ψ. These are currently being investigated with the complete data sample.

In short, the J/ψ data from MARK III has yielded some very interesting results and raised numerous important questions. A very rich analysis program is in progress and promises to address these issues.

For further datataking, the innermost drift chamber (trigger chamber) in the MARK III detector will be replaced by a high precision vertex detector. This will improve trigger efficiency, track resolution and track reconstruction efficiency, in particular for short tracks, while ensuring an efficient background rejection (e.g. cosmic rays). With the expected upgrade in SPEAR luminosity, MARK III will continue to be a source of very rich physics.

References:

1. G. Bhanot, Phys. Lett. 101B,95 (1981); J. F. Donoghue, K. Johnson, B. A. Ali, Phys. Lett. 99B,416 (1981); J. Coyne, P. Fishbane, S. Meshkov, Phys. Lett. 91B, 259 (1980); T. Barnes, Z. Phys. C10,275 (1981).

2. D. L. Scharre *et. al.*, Phys. Lett. 97B,329 (1980); C. Edwards *et. al.*, Phys. Rev. Lett. 49,259 (1982).

3. C. Edwards *et. al.*, Phys. Rev. D25,3065 (1982).

4. D. L. Scharre, Proceedings of the Tenth International Symposium on Lepton and Photon Interactions at High Energy, Bonn (1981).

5. S. Okubo, Phys. Lett. 5,165 (1963); G. Zweig, CERN Preprints CERN-TH-401,402,412 (1964); J. Iizuka, Prog. Theor. Phys. Suppl. 37-38, 21 (1966).

6. T. Appelquist and H. D. Politzer, Phys. Rev. Lett.34,43 (1975); T. Appelquist and H. D. Politzer, Phys. Rev.D12,1404 (1975).

7. M. Chanowitz, Phys. Rev. D12,918 (1975); T. Appelquist, R. M. Barnett, K. Lane, Ann. Rev. Nucl. Sci.28, 387 (1978).

8. F. J. Gilman, in High Energy Physics and Nuclear Structure - 1975, Proceedings of the Sixth International Conference, Santa Fe and Los Alamos.

9. K. Einsweiler, Proceedings of the International Europhysics Conference on High Energy Physics, Brighton, 1983; W. Toki, Proceedings of the 11th SLAC Summer Institute on Particle Physics, July 1983; D. Hitlin, Proceedings of the International Symposium on Lepton and Photon Interactions, Cornell, 1983.

10. M. Chanowitz and S. R. Sharpe, Phys. Lett. 132B,413 (1983).

11. B. F. L. Ward, Phys. Rev. D31,2849 (1985).

12. S. Godfrey, R. Kokoski and N. Isgur, Phys. Lett. 141B,439 (1984).

13. M. Shatz, Phys. Lett. 138B,209 (1984); S. Pakvasa *et al.*, Phys. Lett. 145B, 134 (1984); S. Pakvasa *et al.*, Phys. Rev. D31,2378 (1985).

14. R. M. Baltrusaitis *et al.*, Phys. Rev. Lett. 56,107 (1986).

15. J. F. Donoghue, Proceedings of the International Europhysics Conference on High Energy Physics, Bari, Italy, July 1985.

16. J. Rosner, Proceedings of the Twelfth International Symposium at High Energies, Kyoto, Japan, August 1985, and References therein.

17. J. J. Becker *et al.*, SLAC-PUB-3720, to appear in Phys. Rev.

18. J. J. Becker *et al.*, Contributed Paper to the XXIII International Conference on High Energy Physics, Berkeley, CA, 1986.

19. B. Jean-Marie, Invited Talk at the XXIII International Conference on High Energy Physics, Berkeley, CA, 1986.

20. D. Alde *et al.*, Contributed Paper to the XXIII International Conference on High Energy Physics, Berkeley, CA, 1986.

21. D. Aston, Invited Talk at the XXIII International Conference on High Energy Physics, Berkeley, CA, 1986; B. Ratcliff, Invited Talk at the SLAC Summer Institute, 1986.

22. A. Etkin *et al.*, Phys. Rev. Lett. 49,1620 (1982).

23. R. M. Baltrusaitis *et al.*, Phys. Rev. Lett. 52,2126 (1984).

24. D. Bisello *et al.*, Phys. Lett. 179B,289 (1986); D. Bisello *et al.*, Phys. Lett. 179B, 294 (1986).

25. R. M. Baltrusaitis *et al.*, Phys. Rev. D33,629 (1986).

26. L. Montanet, CERN Report CERN/EP 82-69, Rept. Prog. Phys. 46,337 (1983).

27. S. U. Chung, Phys. Rev. Lett. 55,779 (1985).

28. H. Lipkin, Phys. Lett. 171B,298 (1986).

29. J. D. Richman, Proceedings of the XXth Rencontre de Moriand, Les Arcs, France, March, 1985.

30. P. Baillon *et al.*, Nuovo Cimento 50A,393 (1967).

31. C. Dionisi *et al.*, Nucl. Phys. B169,1 (1980); T. Armstrong *et al.*, Phys. Lett. 146B, 273 (1984).

32. H. Aihara *et al.*, Phys. Rev. Lett. 57,2500 (1986); G. Gidal, Invited Talk at the XXIII International Conference on High Energy Physics, Berkeley, CA, 1986.

33. M. Stanton *et al.*, Phys. Rev. Lett. 42,346 (1979); A. Ando *et al.*, Phys. Rev. Lett. 57, 1296 (1986).

34. J. J.Becker *et al.*, SLAC-PUB-4149, to appear in Phys. Rev. Lett.

35. W. F. Palmer and S. S. Pinsky, Phys. Rev. D27,2219 (1983).

36. M. Frank, N. Isgur, P. J. O'Donnell and J. Weinstein, Proceedings of the International Europhysics Conference on High Energy Physics, Bari, Italy, July 1985.

37. S. Okubo, Phys. Lett. 5,165 (1963).

38. S. Meshkov, W. F. Palmer and S. S. Pinsky, DOE/ER/01545-382; D. Caldwell, Contributed Paper to the XXIII International Conference on High Energy Physics, Berkeley, CA, 1986.

39. M. Chanowitz, LBL-22611.

40. R. M. Baltrusaitis *et al.*, Phys. Rev. D32,2883 (1985).

41. R. Jaffe, Phys. Rev. D15,267 (1977).

42. J. Weinstein and N. Isgur, Phys. Rev. Lett.48,659 (1982); J. Weinstein and N. Isgur, Phys. Rev.D27,588 (1983).

43. K. L. Au, D. Morgan and M. R. Pennington, RAL-85-099 (1985); K. L. Au, D. Morgan and M. R. Pennington, RAL-86-076 (1986).

44. S. M .Flatté, Phys. Lett. 63B,224 (1976).

45. T. Barnes, Phys. Lett. 165B,434 (1985).

46. S. S. Pinsky, Phys. Rev. D31,1753 (1985).

47. A. Seiden, H. F.-W. Sadrozinski and H. E. Haber, SCIPP-86/73.

48. R. M. Baltrusaitis *et al.*, Phys. Rev. D33,1222 (1986).

49. R. M. Baltrusaitis *et al.*, Phys. Rev. Lett. 55,1723 (1985).

50. N. Wermes, Proceedings of the Fifth International Conference on Physics in Collision, Autun, France, July 1985, and SLAC-PUB-3730.